ERDC/CHL TR-22-5

Coastal and Hydraulics Laboratory

US Army Corps of Engineers®
Engineer Research and Development Center

ERDC
ENGINEER RESEARCH & DEVELOPMENT CENTER

Coastal Inlets Research Program (CIRP)

Evaluating Cross-Shore Sediment Grain Size Distribution, Sediment Transport, and Morphological Evolution of a Nearshore Berm at Fort Myers Beach, Florida

Gary A. Zarillo, Sara A. Ramos, Kristopher Effinger, Kristen Becker, Irene Watts, Katherine E. Brutsché, Brian C. McFall, and Douglas R. Krafft

March 2022

The US Army Engineer Research and Development Center (ERDC) solves the nation's toughest engineering and environmental challenges. ERDC develops innovative solutions in civil and military engineering, geospatial sciences, water resources, and environmental sciences for the Army, the Department of Defense, civilian agencies, and our nation's public good. Find out more at www.erdc.usace.army.mil.

To search for other technical reports published by ERDC, visit the ERDC online library at https://erdclibrary.on.worldcat.org/discovery.

ERDC/CHL TR-22-5
March 2022

Evaluating Cross-Shore Sediment Grain Size Distribution, Sediment Transport, and Morphological Evolution of a Nearshore Berm at Fort Myers Beach, Florida

Gary A. Zarillo, Sara A. Ramos, Kristopher Effinger, Kristen Becker, and Irene Watts

Department of Ocean Engineering and Marine Sciences
Florida Institute of Technology
150 West University Blvd
Melbourne, FL 32901

Katherine E. Brutsché, Brian C. McFall, and Douglas R. Krafft

US Army Engineer Research and Development Center
Coastal and Hydraulics Laboratory
3909 Halls Ferry Road
Vicksburg, MS 39180-6199

Final report

Prepared for US Army Engineer Research and Development Center
3909 Halls Ferry Road
Vicksburg, MS 3910-6199

Under Funding Account Code U4362900; AMSCO Code 06000

Abstract

Navigation channels are periodically dredged to maintain safe depths. Dredged sediment was historically placed in upland management areas or in offshore disposal areas. Florida state law prohibits placement of beach fill sediment that contains more than 10% by weight of silt and clay, which is typically a characteristic of dredged material. An alternative is placement in a nearshore berm. Some potential benefits of nearshore berms include wave energy dissipation, reduced cost of dredging and shore protection, and possible onshore movement of the berm material. This study considers sediment distribution, morphological evolution, sediment transport, and shoreline trends along Fort Myers Beach, Florida, related to the nearshore berm constructed in August 2016. Due to timing of the field study, this report also includes information on the influence of a major hurricane that impacted the area. The overall conclusion of this study is that the dredge-sourced sediment in the berm performed as expected. Within 2 years, the berm adjusted to the shoreface environment, maintained a large part of its original volume, and contributed to protection of the beach and shoreline. The impact of Hurricane Irma included a shift in sediment textures and a large but temporary increase in shoreface sediment volumes.

Contents

Figures and Tables

Figures

Tables

Preface

This study was conducted for the US Army Engineer Research and Development Center (ERDC), under the US Army Corps of Engineers (USACE), Coastal Inlets Research Program (CIRP), "Inlet Geomorphological" work unit, Funding Account Code U4362900; AMSCO Code 06000, as part of the USACE Navigation Program. The CIRP is funded by the Operation and Maintenance Navigation Business Line of Headquarters, USACE (HQUSACE). This study was conducted by the Florida Institute of Technology and ERDC, Coastal and Hydraulics Laboratory (CHL), Navigation Division, Coastal Engineering Branch, Vicksburg, MS.

At the time of publication of this report, Ms. Lauren M. Dunkin was chief, Coastal Engineering Branch; Ms. Ashley E. Frey was chief, Navigation Division; Dr. Tanya M. Beck, Coastal Engineering Branch, was CIRP program manager; Ms. Tiffany Burroughs was chief, HQUSACE Navigation Branch and Navigation business line manager; and Mr. Charles E. Wiggins, CHL, was ERDC technical director for Navigation. Dr. Ty V. Wamsley was director of CHL, and Mr. Keith Flowers was deputy director of CHL.

The commander of ERDC was COL Teresa A. Schlosser. The director of ERDC was Dr. David W. Pittman.

1 Introduction

This study is an assessment of a nearshore berm constructed at Fort Myers Beach, Florida, from sediment dredged from nearby Matanzas Pass in the Summer of 2016. Approximately 40% of material dredged by the US Army Corps of Engineers (USACE) is put to beneficial use. Dredged material can be placed outside the littoral system, with very little material placed in the beach or nearshore (Montague 2008). In the case of Fort Myers Beach, dredged sediment was used for berm construction rather than being used as nourishment material since it contained a higher percentage of fine-grained material than allowed to be placed on the beach (State of Florida, Department of State 2010).

1.1 Background

Periodic maintenance dredging of navigation channels is necessary to maintain safe, navigable passage for vessels. The sediment removed through this process often contains a high percentage of fine-grained sediment. Due to this composition, the sediment is not usable for beach nourishment in the state of Florida, which is limited to approximately 2% of fine-grained material for beach quality sand (State of Florida, Department of State 2010). Therefore, in many cases, material dredged from navigation channels must be used in another manner. Historically, disposal methods include either offshore spoil sites or upland disposal. This removal and disposal of channel sediments can exacerbate sand deficits to beaches, dunes, and inlet shoals since these sediments may contain grain size fractions that are compatible with beach and shoreface sediments (Montague 2008).

A more recent approach to disposing of dredged sediment without causing sand deficits is the construction of a nearshore berm. These features consist of placing sediment (which would normally be unusable as direct beach nourishment) in the nearshore where waves will interact and move the sediment. Studies have focused on the benefits of this method (Otay 1994; Smith et al. 2017). Thus, the modern approach to coastal engineering is to utilize dredged material as a resource. In 2016, Matanzas Pass, Florida, was dredged, and the sediment placed offshore in a nearshore berm.

1.2 Objective

In 2016 Matanzas Pass, Florida, was dredged, and the sediment placed offshore in a nearshore berm. The purpose of this study is to analyze the sedimentological and morphological progression of this nearshore berm placed off the coast of Ft. Myers Beach, Florida, and to assess the impacts to the beach and littoral areas. This study can be used to promote the placement of additional nearshore berms in similar environments.

1.3 Approach

This technical report presents the analysis of the sediment distribution, morphological evolution, sedimentological indices, and shoreline trends associated with construction and evolution the experimental 2016 nearshore berm constructed along a section of Ft. Myers Beach, Florida. Topographic survey data were collected and investigated in one-dimensional, two-dimensional, and area-averaged analyses. Volume changes were used to investigate the sediment budget. Sediment samples were collected, and grain size and carbonate content are presented. Statistical sediment differences in time, over the domain, and with elevation were investigated. The impact of Hurricane Irma on changes in morphology and sediment characteristics is discussed. Suspended sediment samples were collected over the water column and are compared across the domain and between sampling dates. Historical shoreline trends were determined from lidar data. Analyses are synthesized to address the project area and placement response.

1.4 Report organization

This report is organized into eight sections and one appendix. Section 1 introduces the purpose and scope of the project. Section 2 provides an overview of physical conditions at the study site and history of the nearshore berm. Section 3 describes field and laboratory methods as well as data analysis methods. Section 4 provides a detailed description of project results, followed by Section 5 in which project results are discussed and synthesized. Section 6 presents a list of conclusions and recommendations to provide guidance for application to similar environments and for future work in the same project area. References are provided in the respective section. The appendix documents morphological changes.

2 Description of the Study Area and Previous Work

2.1 Site description

Fort Myers Beach is located on the Gulf Coast of Florida. This area is classified as a barrier-inlet system and is extensively developed. The beach is located on Estero Island, which is bordered by San Carlos Bay, Big Carlos Bay, and Matanzas Pass (Figure 1).

Figure 1. Geographic setting of the study area. The nearshore berm placement is approximated by the area in red.

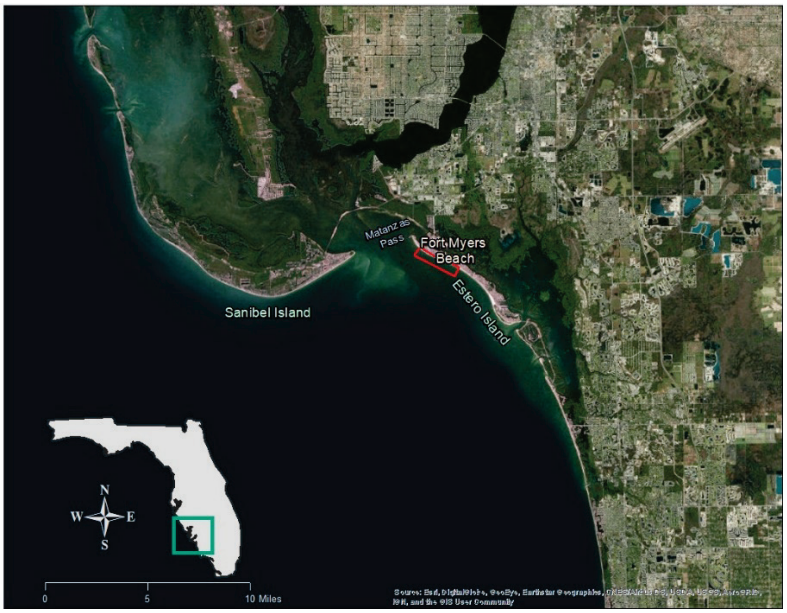

2.2 Meteorological and oceanographic setting

The study area is influenced by a mixed tidal regime. Spring tides are diurnal with a range of approximately 4.0 ft[1], whereas neap tides are semi-diurnal with a range of approximately 2.0–2.5 ft (NOAA 2018).

National Oceanic and Atmospheric Administration (NOAA) station 8725110, located approximately 25 mi south of Estero Island, recorded

[1] For a full list of the spelled-out forms of the units of measure used in this document, please refer to *US Government Publishing Office Style Manual*, 31st ed. (Washington, DC: US Government Publishing Office 2016), 248-52, https://www.govinfo.gov/content/pkg/GPO-STYLEMANUAL-2016/pdf/GPO-STYLEMANUAL-2016.pdf.

an average wind speed of 9 mph from 2005 to 2012 (NOAA 2018). Prominent onshore winds approach from the south-southwest while slightly stronger winds approach from the southeast and northwestern directions with an average speed of 8–9 mph (Brutsché 2011). Sanibel Island shelters Estero Island from some of the stronger northwestern winds. The USACE (USACE 1969, 2012) speculated this sheltering effect on the wave regime is the cause of a longshore drift reversal on north end of Estero Island located approximately 2 mi south of Matanzas Pass.

Wave heights range from 0.32 to 0.98 ft except during extreme weather events (Brutsché 2011).

The project area is subject to frequent tropical storms and passage of cold fronts. Two significant storms occurred during the study period. Hurricane Matthew traveled up the eastern coast of Florida in early October of 2016. During this time, the Fort Myers Page Field Airport (KFMY) recorded sustained winds of 21 kn with gusts up to 41 kn. There was no recorded storm surge associated with this storm in the Fort Myers area (Stewart 2017). Topographic surveys were taken prior to the hurricane in September 2016 and after the hurricane in November 2016. On September 11, 2017, Hurricane Irma more directly impacted the study area by tracking just east of Fort Myers, weakening from a category 3 to a category 2. During this time, the KFMY recorded sustained winds of 50 kn along with gusts up to 73 kn and a total rainfall of 10.6 in. Storm surge was estimated to be between 3 to 5 ft along Fort Myers Beach (Cangialosi et al. 2018). Topographic surveys were taken before the storm and again 2 weeks after Irma passed through the area.

2.3 Geologic settings

The study area was most recently submerged during the late Pleistocene Epoch (2.6 My–11.7 Ky). Estero Island is composed of Holocene quartz-rich sediments classified simply as Holocene (11.7 Ky – present) sediments shown as Qh on the Florida State Geological Map (Figure 2). Holocene sediments are a veneer of fine sediment dominated by wave action and tidal currents, which have removed organic material, leaving mostly quartz and shell material. The quartz material is well sorted and sub-rounded predominantly in the fine to very fine size range

Older formations that may be exposed in the area are the Pliocene age (4.2 – 2.8 Ma) Tamiami formation (USACE 1969; Scott et al. 2002; Missimer 1992) and shelly sands of Pleistocene-Pliocene age designated as TQsu in Figure 2. Like other barrier islands of the modern Florida coast, Estero Island is a wave-built veneer of siliciclastic sediments resting on older carbonate-rich lithified sediments. It is likely that the quartz-rich sediments reached Florida in the mid Tertiary Geologic Period in the littoral environments of earlier shoreline and have been subsequently recycled into modern shorelines (Hine 2013; White 1970).

Figure 2. Geological map of Fort Myers area. Core location shown as dot.

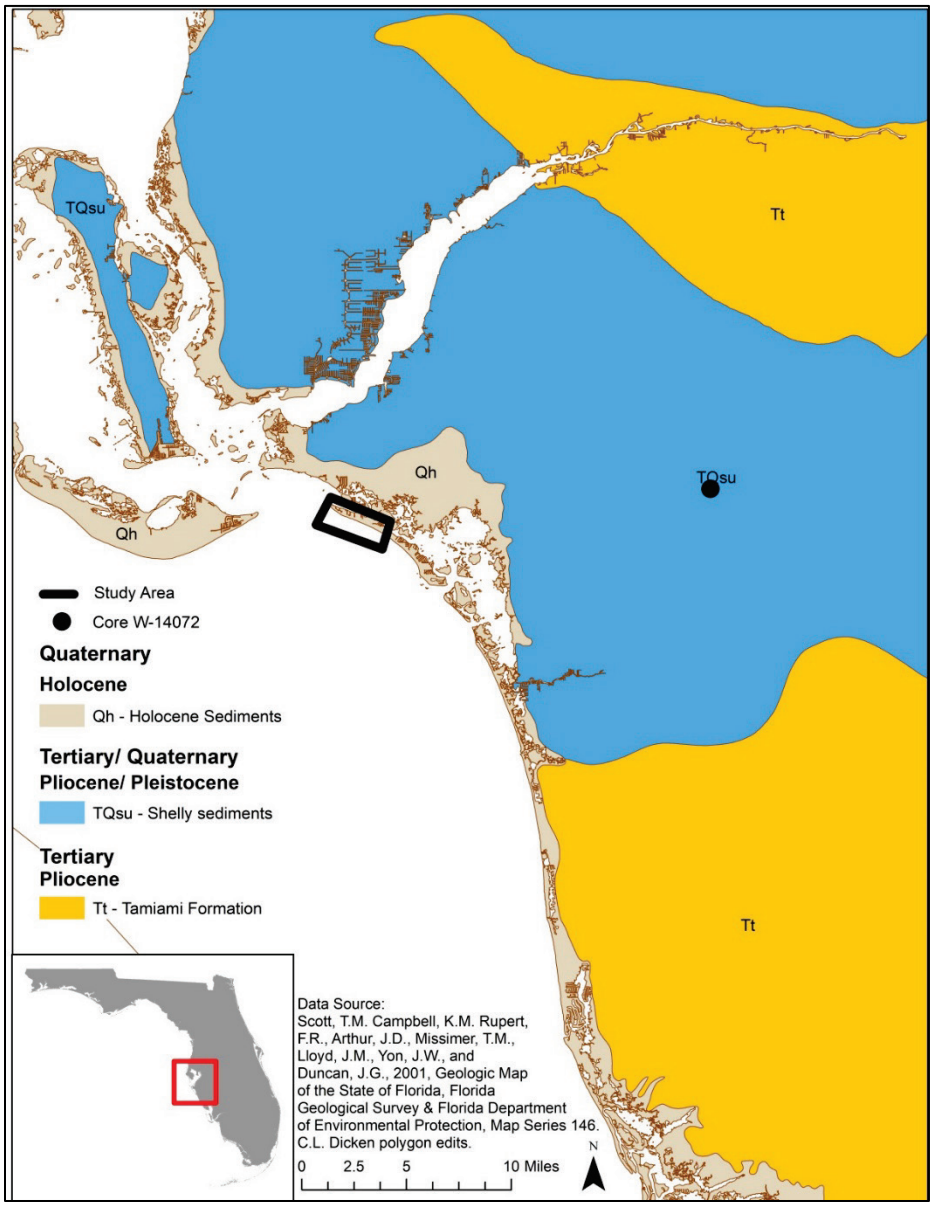

The Fort Thompson Formation ranges from 6 ft to 80 ft thick and is generally described as alternating fresh and brackish-water marine shell marls and limestones (Sellards 1919). Near the study area, it comprises the top 20 ft of core W-14072 and is described as containing medium- to fine-grained quartz sand having up to 15% fine-grained sediments (Missimer 1992). This formation is not officially named on geological maps but is likely associated with the TQsu unit of shelly sediments (Figure 2).

The Tamiami Formation is also found in the region and contains a wide range of mixed carbonate, clastic, and fossil assemblages and often described with at least nine facies having various specific compositions and thicknesses at a given location. Core (W-14072) data near the study site suggest that the top of the Tamiami Formation is comprised of limestone with a moldic porosity and variable percentages of sand (Missimer 1992).

2.4 Previous coastal engineering work

In 1969, the USACE (1969) conducted a beach erosion control study in which it examined littoral sediment characteristics and littoral transport patterns. The USACE determined the median grain size for Estero Island ranged from 0.14 mm in the beach dune area to 0.27 mm at -12 ft depth (USACE 1969). This earlier study represents the native beach sediment.

The 1969 study results indicated that longshore transport within Estero Island was predominantly southward at a rate of approximately 66,000 yd^3 annually and is consistent with the regional trend with the exception of the northern-most section of the island, along which net longshore sediment transport may move northward. It was determined that the reversal occurs approximately 2 mi south of the tip of Estero Island at an estimated annual transport rate between 12,000 yd^3 and 22,000 yd^3. A more recent study conducted by Coast and Harbor Engineering (2015) placed this reversal slightly north of the 1969 report at an annual transport rate of 22,900 yd^3 along the northern section of Estero Island. Both studies agree that the location of reversal can change throughout the year. The above sediment transport rates are considered averages and do not account for major storm events.

The northern section of Estero Island has been renourished several times since 1960, with most of the renourishment occurring between R-178 and R-180 (Figure 3). Table 1 shows a summary of all beach renourishment projects including amounts deposited and location. Most of the sediment was dredged from Matanzas Pass with the exception of 2017 and 2011 when fill material was derived from either offshore or upland sources (Coast & Harbor Engineering 2015). The most recent direct beach nourishment is the only event that directly affects this study.

Figure 3. Location of most recent beach renourishments and associated R-markers.

After the effects of Hurricane Irma in September 2017, an emergency order from the Florida Department of Environmental Protection (FDEP) authorized a renourishment within the study area. In September of 2017, approximately 2,100 yd^3 of material from an upland mine was placed within crescent beach Family Park between Range Markers 181 and 182 (Figure 3).

Table 1. History of direct beach nourishment on Estero Island. Modified from Coast & Harbor Engineering (2015).

Date	Volume ((cy))	Placement
2/1961 to 3/1961	265,000	R-178.2 to R-180.5
8/1961 to 11/1961	52,000	R-178.2 to R-180.5
1972	110,000	R-178.2 to R-180.5
11/1979 to 4/1980	192,000	R-178.2 to R-180.5
10/1982 to 10/1983	71,000	R-178.2 to R-180.5
11/1985 to 6/1986	96,000	R-178.2 to R-180.5
4/1996 to 5/1996	188,712	R-179.1 to R-183.7
2001	187,800	R-178.2 to R-185.5
2009	229,313	R-182 to R-187A
2011	402,805	R-174.6 to R-181.5
2016	130,000	R-182 to R-187A
11/2017 to 12/2017	2,096	R-181.2 to R-181.5

2.5 Nearshore berm history

Matanzas Pass is a federally maintained channel used for recreation and passage to the United States Coast Guard station. This channel requires frequent dredging to maintain a safe navigation depth. In July 2009, instead of removing the dredged material from the littoral system, the USACE began a repeated cycle of using the dredged material to construct an active nearshore berm at Ft. Myers Beach, Florida.

Prior to placement of the 2009 berm, the USACE surveyed the area to establish baseline hydrographic and topographic conditions. Starting April 2010, Brutsché (2014) surveyed eight times within 3 yr. Brutsché (2014) used cross-shore profiles to determine that the berm had reached a natural equilibrium state by 2013. This was determined by comparing the average variances from the equilibrium profile to the associated standard deviations at the south control area.

The 2009 nearshore berm was constructed in four stages. The first stage consisted of equipment deployment. Stage two and four were dredged from the Cut-2a (Figure 4) and contained an average grain size of 0.18 mm. It was deposited rapidly in the northern section of the nearshore berm and resulted in a narrow berm with gaps less than 50 ft wide and varying berm heights. Stage three was dredged from Cut-1 and

contained an average grain size of 0.16 mm. This material was placed farther south, more slowly, and resulted in a broader berm. In total, approximately 230,000 yd^3 of material was placed in approximately 6 ft water depth (NAVD88), was approximately 6,000 ft long, 400 ft wide, and 3 ft high (Brutsché 2011). Brutsché (2014) indicated that this placement reached dynamic equilibrium in fewer than 4 yr.

In July 2016, the USACE again used material dredged from Matanzas Pass to construct a nearshore berm at Ft. Myers Beach. Material was dredged from not only Cut-1 but also Cut-3 (Figure 4); 125,500 yd^3 of material was dredged from Cut-1, and 10,000 yd^3 was dredged from Cut-3. The completed berm was placed at approximately 6 ft water depth (NAVD88) and was approximately 3,000 ft long, 400 ft wide, and 3 ft high.

Figure 4. Placement location of nearshore berm, dredging sites, and extent of north control area, nearshore berm area, and south control area.

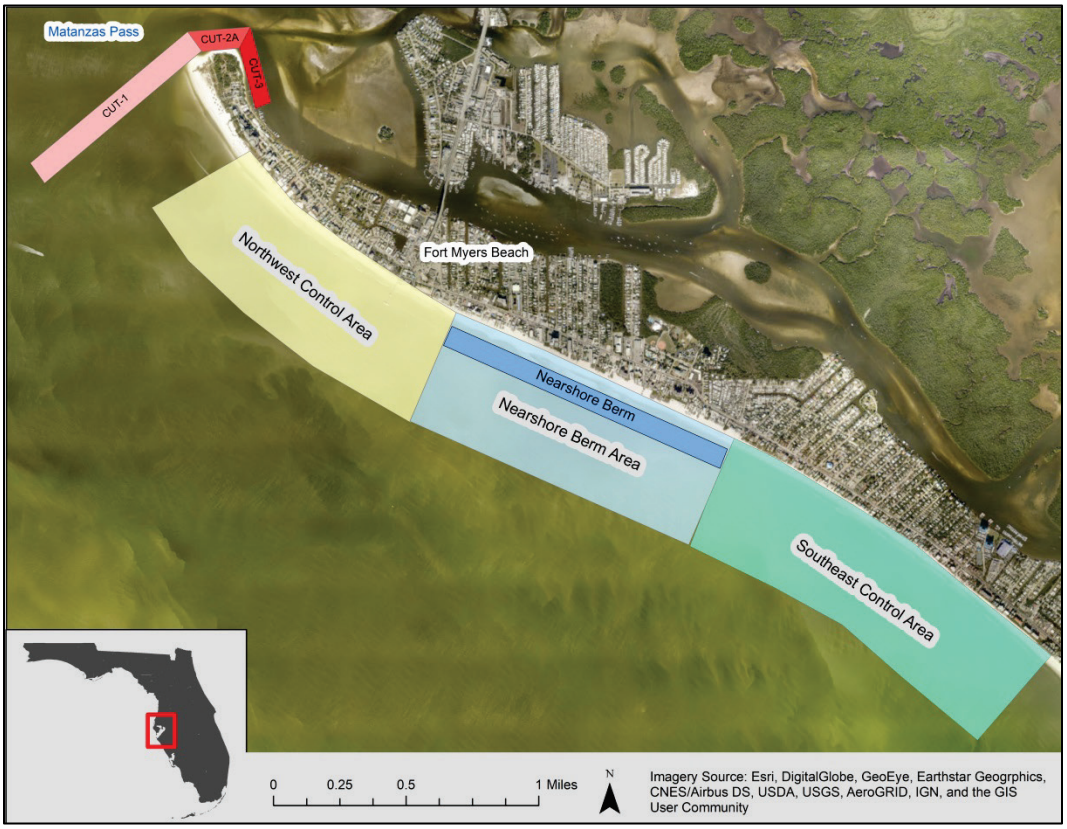

2.6 Shoreline change studies

In December 2011, a beach nourishment and terminal groin were placed on the northern tip of Estero Island. After construction, the FDEP requested monitoring to determine effects of the groin on the local sediment budget. Coastal Engineering Consultants, Inc. surveyed the northern section of the island. The study reported that individual beaches within its study area showed high variability between volume gain and loss. Between 2012 and 2015, the northern section of its study area (monument R-175 and C-174A) showed that the shoreline advanced at a rate of 14.9 ft/yr. In contrast, the shoreline recessed -21.6 ft/yr between monuments R-175 and R182 and accreted 11.8 ft/yr between monuments R-183 and R-186. On average, the shoreline receded at an annual rate of approximately 0.3 ft between July 2014 and June 2015 (Coastal Engineering Consultants, Inc. 2015). End point rate (EPR) calculations were performed for the overall years of 1998 to 2015, prior to berm construction 1998 to 2007, and after berm construction 2007 to 2015.

The EPR method was applied using the Esri ArcGIS desktop Digital Shoreline Analysis System (DSAS), which uses the first and last shoreline point to determine changes (Himmelstoss et al. 2018). Previous studies have shown that this area is prone to high variability, and therefore the EPR approach provides an accounting of the trend of net shoreline change but does not account for variability between survey data sets.

As documented in Table 1, multiple beach nourishment projects were constructed within the study area between 1998 to 2017. Event-scale shoreline changes from both storms and nourishment projects can influence the average shoreline trends in the areas. Thus, when interpreting shoreline changes with respect to long-term stability, care must be taken to consider the time scale over which shoreline imagery is available.

3 Methods

Topographic and sedimentological data were collected on and around the berm to determine the morphological evolution and sediment movement associated with the berm. Data collection methods include multiple topographic surveys of the beach and shoreface, two sets of bottom sediment samples, and two sets of suspended sediment samples, as well as near-bed sediment samples to characterize bedload sediment characteristics. Processing of field data included analysis of grain size distributions, sediment composition in terms of carbonate content, and topographic data were used to observe the evolution of the constructed berm and estimate a sediment budget for the project area. In addition to the topographic surveys, a shoreline change analysis was conducted based on historical lidar data and a recent field survey to document the overall stability of the shoreline through the project period.

3.1 Topographic surveys

Topographic surveys (Figure 5) were conducted by the USACE in August 2016, September 2016, and November 2016 directly after placement of the 2016 nearshore berm. Under this project, additional surveys were conducted in May 2017, August 2017, September 2017, and January 2018 by the Florida Institute of Technology Coastal Processes Research Group (CPRG). Both groups used similar methods in field data collection, and therefore the resulting elevation data from both groups are comparable.

3.1.1 Topographic data collection

During the 2016 collection period, elevation was collected by the USACE on 57 transects matching the original transects set up during the 2009 berm project from approximately +5 ft to -15 ft (NAVD88). Additionally, the beach was surveyed using terrestrial lidar in September 2016 and November 2016 from the toe of the vegetated dune or private property line if absent to the beach swash line.

In May 2017, August 2017, September 2017, and January 2018, topographic surveys were collected by CPRG. Topographic information was collected on 72 transects, which included the original 57 transects from previous studies, and extended from the toe of the vegetated dune

to the -10 ft contour (Figure 5). Elevations were georeferenced to the State Plane Florida West coordinate system (Zone 0902) and the NAVD88 vertical datum.

Figure 5. Location of topographic transects collected by USACE and CPRG in reference to location of nearshore berm, north control area, nearshore berm area, and south control area.

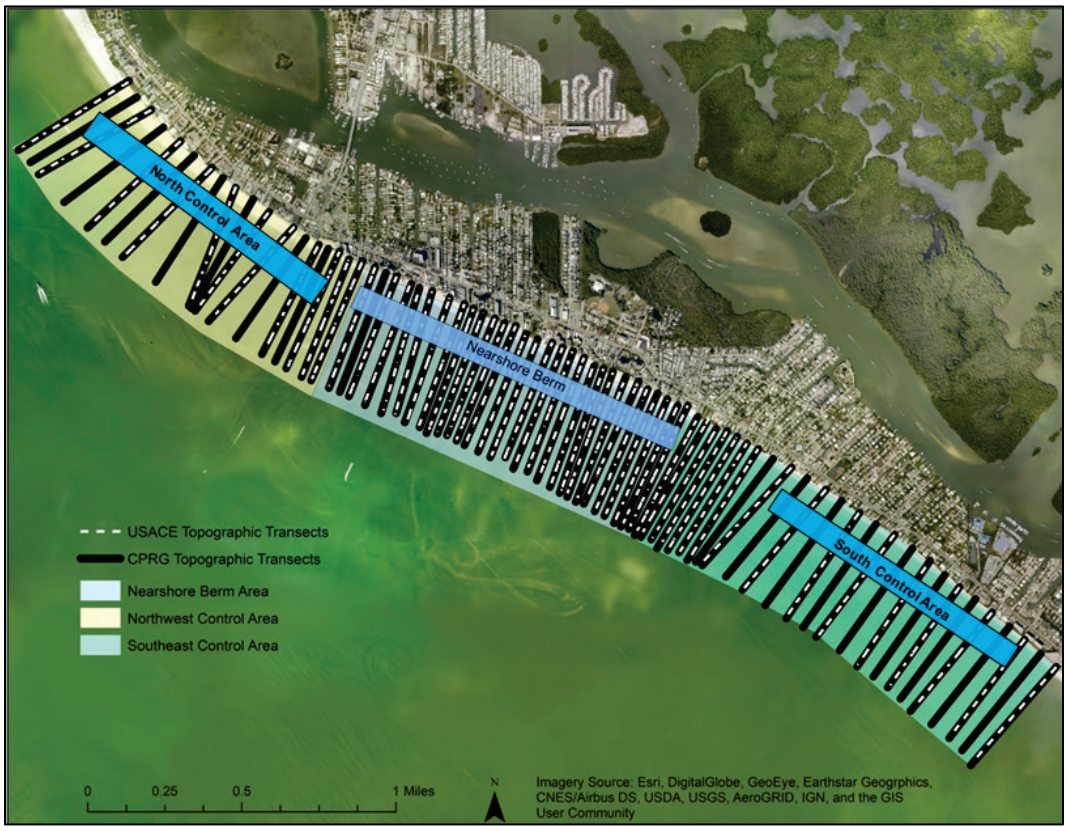

Shallow areas, including dry beach to approximately -4 ft elevation, were surveyed using a Real-time kinematic (RTK) global navigation satellite system (GNSS) unit using a point density of approximately 10 ft. The RTK GNSS rover was used in conjunction with a data logging unit and cell phone hotspot to collect with a horizontal accuracy of 1–2 cm and a vertical accuracy of 2–3 cm.

Deeper areas (-3 ft to -10 ft) were collected with a Lowerance HDS-7 Gen3 transceiver and 200 kHz single beam transducer. An onboard accelerometer corrected for error due to the roll, pitch, and heave of the vessel.

3.1.2 Topographic data processing

Survey data were visually inspected to determine the accuracy of conjoining the topographic and bathymetric profiles, as some locations showed an elevation offset between data types. This was most apparent where the RTK GNSS data overlapped the Lowerance single-beam data. To correct for this offset, a Fortran program was created to apply a correction factor to the offshore survey data after an initial tidal and low-frequency sea-level correction was applied. The tidal correction was applied using the predicted tides for nearby Estero Bay to adjust the offshore survey data for tidal stage. This was followed by a final correction to the NAVD88 vertical datum using data from NOAA station 8725520, to which a low pass digital filter was applied to extract the non-tidal sea-level signal.

One-dimensional topographic profile analyses were conducted on nine transects, three for each control area (north, berm, and south control areas). These analyses used data from the USACE collections and the CPRG collection periods. The August 2016 survey was considered a baseline survey representing post-construction conditions with the assumption that very little change occurred during the month between construction and the survey. To determine specific changes associated with the nearshore berm, each profile analysis focused on changes occurring within 1,000 ft from the vegetation line.

A topographic surface was interpolated across the profile data to determine areas of erosion or accretion associated with the berm. Next, the data were combined and corrected to the NAVD88 vertical datum, and the data were further interpolated using the natural neighbor spatial interpolation method. This method applies a weighting factor based on the closest sample locations without inferring trends in the data (ESRI 2016). A grid of evenly spaced points was then used to collect elevation data for each time period. Finally, the surface difference between collection periods was visualized as a Triangulated Irregular Network to highlight areas of erosion or accretion between collection periods. This process was based on previous studies for Sebastian Inlet, Florida (Zarillo et al. 2015). Difference calculations were completed for the periods of August 2016 to September 2016, September 2016 to November 2016, November 2016 to May 2017, May 2017 to September 2017, September 2017 to January 2018, and August 2016 to January 2018.

Volume change analyses were also performed to determine changes in the berm volume during the collection periods. A mask was created to isolate the berm by using profile analysis and referral to a drawing of the proposed berm location. Volume calculations included all space between a base level and surface within the berm mask. An arbitrary base level of -10 ft was used for all calculations to ensure there was no error caused by an insufficient base level. Volume calculations were performed for the masked area over all collection periods (August 2016 through January 2018).

3.2 Sediment data collection and analysis

Sediment samples were collected and processed by Florida Institute of Technology CPRG in May of 2017, September 2017, and again in January 2018. The following sections explains the methodology

3.2.1 Field data collection

The study area was divided into three sections: the north control area, the nearshore berm area, and the south control area. The nearshore Berm area was determined according to the physical placement of the berm whereas the north and south control areas extended from the berm area to the ends of the study area (Figure 4).

Sediment samples collected May 2017, September 2017, and January 2018 by the CPRG were located in correlation with topographic profile data. Samples were collected on every other transect, which included the original 11 transects collected by the USACE as well as an additional 27 transects established by the CPRG. The average spacing between transects with sediment collection was 300 ft within the berm area and 600 ft in the control areas (Figure 6). Sediment samples were collected every two vertical feet (according to NAVD88) with additional samples at the above-mentioned morphological features to ensure replicate samples of the previous collection by the USACE. In total, CPRG collected and processed 807 total sediment samples over three collection periods. Table 2 lists the sample types and numbers by transect.

During the months of May 2017 and January 2018, suspended sediment samples were collected contemporaneously with sediment samples on every third transect, spaced 450 ft within the berm area and 900 ft in

the control areas. Sample locations were chosen to represent the landward, crest, and seaward sides of the berm. Approximately 500 ml water samples were collected just below the surface, at middle-depth, and near-bottom (-2 ft, -4 ft, and -8 ft, respectively) for a total of 216 samples. Samples were collected using a Niskin bottle at -8 ft and by free diving using handheld plastic bottles at -2 ft and -4 ft. It is noted that sediment resuspension may have been exacerbated at -2 ft and -4 ft due to personnel interacting with the bottom during sample collection.

Figure 6. Collection sites for sediment and suspended load.

3.2.2 Laboratory methods

Sediment samples were oven dried and split samples down to approximately 50 g. The samples were then wet-sieved thorough a #230 sieve to remove any fine material less than 4 Phi and once again dried. They were then dry-sieved using a 1/2–phi size interval nest of sieves from 16.00 mm (-4.00 Phi) to 0.06 mm (4.00 Phi). A high-temperature burn method was used to determine the carbonate content of each. This method involves igniting a pre-weighed sample at 1,080 °C for 8 hr.

Table 2. Samples collected according to transect number.

Transect Number	USACE Sediment Samples	CPRG May Sediment Samples	CPRG May Suspended Samples	CPRG Sept Sediment Samples	CPRG Jan Sediment Samples	CPRG Jan Suspended Samples
FMF1		8			8	
FMF2			9			9
FMF3		8			8	
FMF5	5	11	9	11	11	9
FMF7		7			7	
FMF8			9			9
FMF9		8			8	
FMF11	4	11	9	11	11	9
FMF13		7			7	
FMF14			9			9
FMF15		8			8	
FMF17	7	11	9	11	11	9
FMF19			9			9
FMF20		8			8	
FMF22	6	10	9	10	10	9
FMF24		8			8	
FMF25			9			9
FMF26	4	12		12	12	
FMF28		8	9		8	9
FMF30		8			8	
FMF31	4	12	9	12	12	9
FMF32		8			8	
FMF34		8	9		8	9
FMF36		8			8	
FMF37	5	12	9	12	12	9
FMF38		8			8	
FMF40		8	9		8	9
FMF42		8			8	
FMF43			9			9
FMF44	3	14		14	14	
FMF45						

Transect Number	USACE Sediment Samples	CPRG May Sediment Samples	CPRG May Suspended Samples	CPRG Sept Sediment Samples	CPRG Jan Sediment Samples	CPRG Jan Suspended Samples
FMF46		8	9		8	9
FMF48		8			8	
FMF49			9			9
FMF50		8			8	
FMF52		8	9		8	9
FMF54	7	13		13	13	
FMF55			9			9
FMF56		7			7	
FMF58		7	9		7	9
FMF60		8			8	
FMF61			9			9
FMF62		8			8	
FMF64	5	11	9	11	11	9
FMF66		8			8	
FMF67			9			9
FMF68		8			8	
FMF70	7	10	9	10	10	9
FMF72		8			8	

During ignition, the carbonate (calcite) crystal lattice is broken down, carbon dioxide released, and only the calcium atoms remain. Thus, the weight percent carbonate can be calculated knowing the atomic weights of the atoms forming the calcite lattice. The carbonate analysis methodology is described in Heiri et al. (1999)

The basic sediment grain size data were compiled in the gINT© geotechnical software platform and exported into standard graphic plots of grain size distribution along with associated data tables in spreadsheet format. Calculation of grain size statistics was according to the method of moments. From the basic data set, the sediment data were partitioned into the various graphical and statistical analyses.

Suspended sediment samples were processed through 0.45 micron filters using a Millipore filtering system. Processing includes filtering of

the 500 ml mixtures of sediment and water, filtering, drying, and weighing to a precision of 0.001 g.

3.2.3 Sediment size distribution

Sediment grain size distributions determined from the samples collected during three of the four survey periods were examined for spatial and temporal changes. Sediment abundance according to weight percent were combined into eight groups of size classes ranging from silt to coarse sand and two categories consisting of fine shell fragments and coarse shell fragments. These groups were then examined for abundance according to the north control area, berm area and south control area, as well as being examined according to the elevation of the sample location across the beach and shoreface. The goal of the spatial and temporal grain size analysis was to determine if the size distribution of sediments placed in the Berm changed over time and space as the berm morphology adjusted to the shoreface environment.

In addition to analysis of bottom grab samples over the project area, suspended sediment sample data were examined for spatial and temporal variations in concentration to determine if recognizable concentration differences could be observed among the project north, berm, and south areas and among the cross-shore s positions of the samples. A question to be answered is whether the sediments placed in the berm area have an influence on sediment concentration in the water column above.

3.2.4 Statistical analyses

Statistical testing of sediment grain size statistics was conducted to complement and confirm the spatial and temporal analysis of grain size distribution over the project area. Two phases of statistical hypothesis tests were conducted. The first phase determined if the modal sediment grain size was statistically different between collection times (May 2017, September 2017, and January 2018), areas (north control, south control, and berm locations), and elevations (+4, +2, 0, -2, -4, -6, -8, and -10 ft). The modal grain size was chosen to represent the central tendency of the sample populations because they were not normally distributed but were instead negatively skewed (toward the coarse tail). Other measures of central tendency such as the mean and median diverge from the mode in skewed non-normally distributed samples. In

this case, the mode (most abundant sediment size class) was considered the best single representative sample statistic.

The second phase focused on the percent of fine-grain material (<0.06 mm) within the -4 ft and -2 ft elevations. This depth and sediment size was chosen to best represent the percent of fine-grain material directly associated with the berm. This phase determined if the percent of fine-grain material was statistically different throughout the study area between collection times (May 2017, September 2017, and January 2018), areas (north control, south control, and berm locations), and elevations (-4 and -2 ft).

Consequently, in both phases the Kruskal-Wallis test and the Scheirer-Ray Hare test were used to determine the likelihood that changes in sediment characteristics (modal grain size, and percent of fine-grain material) were not due to chance. During all tests, the null hypothesis states that sediment populations within the given time, area, or elevation were equal. This is tested by comparing the p-value to an alpha value. In situations where the p-value was less than the alpha value, the null hypothesis was rejected, concluding that changes in the sediment population were not due to chance.

The Kruskal-Wallis test, which is a non-parametric version of the one-way Analysis of Variance (ANOVA), was used to test changes in collection times (Sokal and Rohlf 1995). Time represents the collection periods of May 2017, September 2017, and January 2018. Some variability due to seasonal changes was expected, but overall average grain size is expected to remain similar throughout this short amount of time; therefore, the null hypothesis is that grain size is equal during these time periods. The standard alpha value of 0.05 was used to test at the 95% confidence level. With resulting p-values smaller than 0.05, the null hypothesis was rejected and it is stated that sediment changes are not due to chance, and therefore at least one time period is different from at least one of the others. After rejecting the null-hypothesis, further post-hoc testing was completed to compare pair-wise differences between the time periods determining where the differences occur.

Additionally, the Scheirer-Ray Hare test, an extension of the Kruskal-Wallis test for a Two-Way ANOVA, was used to determine the likelihood that samples taken from each area and elevation came from the same

population (Siegel and Castellan 1988). The variable area refers to the north control area, berm area, and south control area. Each area comprises similar depths and depositional environments therefore it is expected that sediment grain size is similar within all three areas. Elevation refers to sediment collected at specific elevations (+4, +2, 0, -2, -4, -6, -8, and -10 ft). It is anticipated that sediment grain size varies between these elevations. The Scheirer-Ray Hare test also includes analysis for the interaction between area and elevation (Area*Elevation). This variable states that the effect of one variable depends on the value of the other variable. This interaction variable is included in the result section for completeness but is not otherwise discussed here. Because the Kruskal-Wallis showed statistical differences between the collection periods, the Scheirer-Ray Hare test was conducted separately for each collection period with a Bonferroni correction to reduce type II errors (false negatives). Due to the Bonferroni correction, a p-value of 0.025 was used to test at the 97.5% confidence level.

Further post-hoc testing was conducted to isolate pair-wise differences between the two groups (collection periods and areas). The Dunn's post-hoc test was chosen because it is a non-parametric alternative to the Tukey (Siegel and Castellan 1988). This test focused on differences between the collection periods and areas. Traditional post-hoc testing (such as the Dunn's test) was not conducted in reference to elevation. Instead, a graphical representation showing changes in grain size for each elevation were used to better represent changes at individual elevations.

3.3 Shoreline change analysis

Shoreline change analysis was conducted using the Digital Shoreline Analysis System (DSAS v.4.4) within ArcGIS. The DSAS allows the user to calculate the rate of change of shoreline movement by inputting multiple historical shoreline positions (Thieler et al. 2009), which were determined from 1998, 2004, 2006, 2007, 2010, 2012, and 2015 historical lidar data sets. Sources of lidar surveys include the US Geological Survey, the National Atmospheric and Space Administration, and the Florida Division of Emergency Management.

To do so, the zero contour line relative to NAVD88 representing sea level was extracted for each data set and input into DSAS v.4.4 to

create rate-of-change statistics. Transects were cast every 328 ft off an arbitrary baseline. The shoreline rate of change was then calculated using the End Point Rate, EPR method. The EPR is a technique that is based on dividing the distance of the shoreline movement by the total amount of time between all the shorelines provided.

A final step in the shoreline change analysis was to make a comparison of study area shorelines pre- and post-construction of the 2016 berm. The comparison is made between the 2015 NAVD88 zero contour shoreline as seen in the 2015 lidar data and the NAVD88 zero contour shoreline extracted from the January 2018 topographic survey conducted for this study. The methods of comparison were similar to those applied to the historical lidar data sets. Transects were cast from a single baseline to both the 2015 and 2018 shorelines, and the difference between the shoreline positions on the survey dates were calculated and presented graphically.

4 Results

4.1 Sediment grain size distribution

Sediment deposition is largely dependent on hydrodynamic conditions in which coarser sediments are more stable in higher energy environments and finer grain sizes are more stable in lower energy environments. Because of this relationship, an effective way to study how sediment moves in relation to the nearshore berm is to analyze sediment grain size distribution throughout the study area and over time. This study analyzes sediment samples collected in the berm and control areas to determine how sediment deposited within the nearshore berm is moving throughout the study area. Table 3 summarizes the average occurrence by weight of sediment size classes by topographic elevation and collection date. Percentages are provided for sediment in silt to coarse sand size classes, along with the content of carbonate shell material in the fine and coarse ends of the sediment size distribution

The cross-shore distribution of sediment size classes averaged over the north area, berm area and south areas is summarized for each of the survey dates in Figure 7, Figure 8 and Figure 9. As listed in Table 3, the most notable differences among the three survey dates occurred in the finer most abundant sediment size classes, including fine sand (0.125––0.250mm), very fine sand (0.06––0.125mm), and silt (<0.06 mm), fractions.

Figure 7 compares the cross-shore distribution of sediment sizes by depth in the north area for all three sampling periods. The fine sand and very fine sand size classes dominate the sediment distibution but vary in their relative percentages among the survey dates, particulaly at depths greater than -2 ft. Between the May 2017 and September 2017 surveys, the percent silt fraction at -10 ft increased from approximately 5% to 20% along with an increase of approximately 20% in the very fine sand fraction at this depth. A marked increase in the very fine sand fraction also occurred at the -4 ft bethynetric location. Since the results are in terms of weight percent, increase in one size class corresponds to decrases in other size classes, which is the essense of a closed data set. Thus, the balance is largely between the most abundant fine and very fine sediment classes.

Table 3. Average percentages of grain size classes by date and elevation.

	Elevation. (ft)	Silt	Very Fine Sand	Fine Sand	Med Sand	Coarse Sand	Very Coarse Sand	Fine Shell	Coarse Shell
May 2017	4	1.7	17.8	76.7	2.3	0.9	0.3	0.1	0.2
	2	2.1	16.8	79.7	0.7	0.2	0.1	0.1	0.3
	0	0.2	22.6	62.8	6.3	3.4	2.5	1.3	0.9
	-2	5.7	28	52.6	4.3	3.3	2.6	1.8	1.6
	-4	6.9	40.6	46.3	2.7	1.6	0.8	0.5	0.6
	-6	7.3	52.8	37.2	1.1	0.7	0.4	0.2	0.3
	-8	26	39.2	31.3	1.7	0.9	0.5	0.2	0.2
	-10	23.1	37	32.2	2	1.2	0.9	0.6	2.9
	Average	**9.1**	**31.9**	**52.4**	**2.6**	**1.5**	**1.0**	**0.6**	**0.9**
Sept. 2017	4	0.9	22.7	73.2	1.9	0.9	0.2	0	0.2
	2	6.3	22.4	61.9	5.9	1.6	1	0.4	0.4
	0	1.5	24.3	56.9	5.2	4.2	3.7	2.3	2
	-2	1.5	35.6	56.3	2.9	1.4	1	0.5	0.9
	-4	2.1	60.5	35.4	1.1	0.4	0.2	0.1	0.1
	-6	3.8	60.4	32.7	1.2	0.7	0.5	0.3	0.5
	-8	1.2	47.3	46.5	1.9	1.3	0.9	0.3	0.5
	-10	21.2	43.4	27	2.3	1.7	2.1	1.1	1.2
	Average	**4.8**	**39.6**	**48.7**	**2.8**	**1.5**	**1.2**	**0.6**	**0.7**
Jan. 2018	4	1.6	15.5	78.1	2.3	1.1	0.8	0.3	0.3
	2	2.1	15.4	78.2	2.7	0.8	0.4	0.1	0.2
	0	1.7	23.4	54.2	5.7	7	5.2	1.7	1.3
	-2	1.6	32	58.4	2.1	1.7	1.6	0.8	1.8
	-4	2	44.1	47.5	1.9	1.7	1.3	0.5	1.1
	-6	2.1	54.6	39.7	1.5	0.8	0.6	0.2	0.4
	-8	13.9	36.7	40.4	2.3	2	2.3	1.2	1.3
	-10	19.5	28	40.9	3.4	2.7	2.5	1.6	1.4
	Average	**5.6**	**31.2**	**54.7**	**2.7**	**2.2**	**1.8**	**0.8**	**1.0**

As seen in Figure 7, the abundance of the very fine sand size class in the north control area decreased at -8 and -10 ft along with a decrease in silt content to about 5% at -10 ft in January 2018. Fine sand was the most abundant size class at all depths in January. Another pattern in the January 2018 results was a wider overall size distribution into the coarser size classes at depths of 0 ft and below compared to the two earlier surveys, although the abundance of the coarser size classes remained low.

Figure 7. Average percent of sediment by size class in the north control area based on the May (A), September 2017 (B), and January 2018 (C) surveys Silt (<0.06 mm), very fine sand (0.06–0.125 mm), fine sand (0.125–0.250 mm), medium sand (0.25–0.50 mm), coarse sand (0.50–1.0 mm), very coarse sand (1.0–2.0 mm), fine shell (2.0–4.0 mm), coarse shell (>4.0 mm) (Ramos and Zarillo 2019).

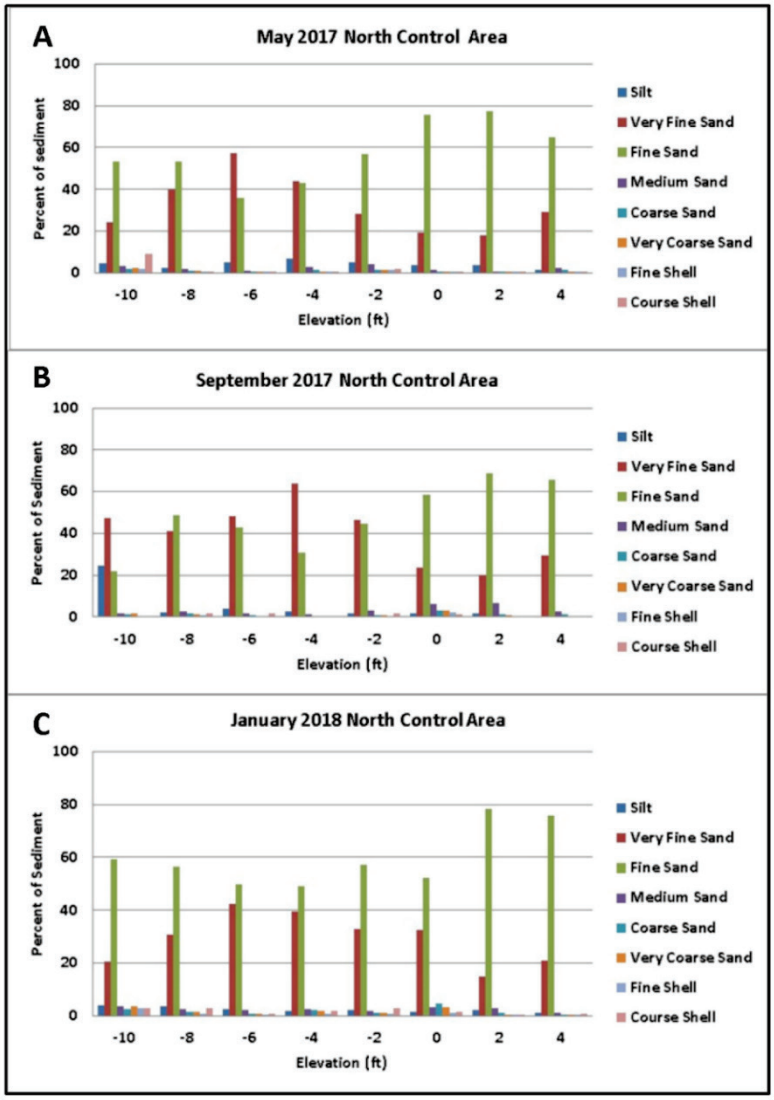

Figure 8 shows the cross-shore sediment distribution in the berm area for each of the sediment survey dates. Overall, the berm area contains higher percentages of silt and very fine sand though all three sampling periods compared to the north control area (Figure 7). Similar to the north control area, the January 2018 results in the berm area included a wider overall size distribution into the coarser size classes at most depths compared to the two earlier surveys. The widest sediment size distribution in all three surveys in the berm area occurred at the 0 ft depth location, which may indicate a cross-shore mixing zone as sediment continually adjusts to dynamic equilibrium. Of particular note is the presence of relatively high percentages of silt at depths of -2 to -10 ft in the May 2017 sediment survey. Percentages of very fine sand dominant at depths of -4 to -10 ft. In the post Hurricane Irma September 2017 survey, the overall relative percentages of very fine sand increased, particularly at depths of -4 ft and greater. Conversely the percentages of fine sand declined at all sampling depths except -8 ft. However, the relative percentages of silt decreased at all depths. In the final January 2018 sediment survey, the cross-shore sediment size distribution shifted to be similar to the July 2017 sediment results, with the exception of silt, which remained low or nearly absent at all depths except -8 and -10 ft.

Figure 9 shows the cross-shore sediment size distribution in the south control area, which displays some fundamental differences compared to the north control area and berm area. The most observable difference was the high abundance of very fine sand and silt at -8 and -10 ft. Silt concentration remained in the 30% to 60% range through all three sediment surveys at -8 and -10 ft. Very fine sand was the most abundant size class at -6 ft throughout the surveys. Sediment distribution at depths of -2 ft and shallower was characterized by high abundance of fine sand and more consistent with the sediment distribution in the berm area and north control areas. Wider sediment size distributions indicating cross-shore mixing of sediment are more apparent in the final January 2018 survey of the south control area, similarly to sediment results from the north and berm areas. A broader sediment distribution is particularly apparent at -8 and -10 ft in the January 2018 south control area. At shallower depths, the noticeable mixed sediment size locations shifted from -2 in the May 2017 survey data to a depth range 0 to +2 ft in the September 2017 survey. In the January 2018

survey of this area, the mixed size sediment zone was most apparent at the 0 ft sample location.

Figure 8. Average percent of sediment by size class in the berm area based on the May (A), September 2017 (B), and January 2018 (C) surveys. Silt (<0.06 mm), very fine sand (0.06–0.125 mm), fine sand (0.125–0.250 mm), medium sand (0.25–0.50 mm), coarse sand (0.50–1.0 mm), very coarse sand (1.0–2.0 mm), fine shell (2.0–4.0 mm), coarse shell (>4.0 mm) (Ramos and Zarillo 2019).

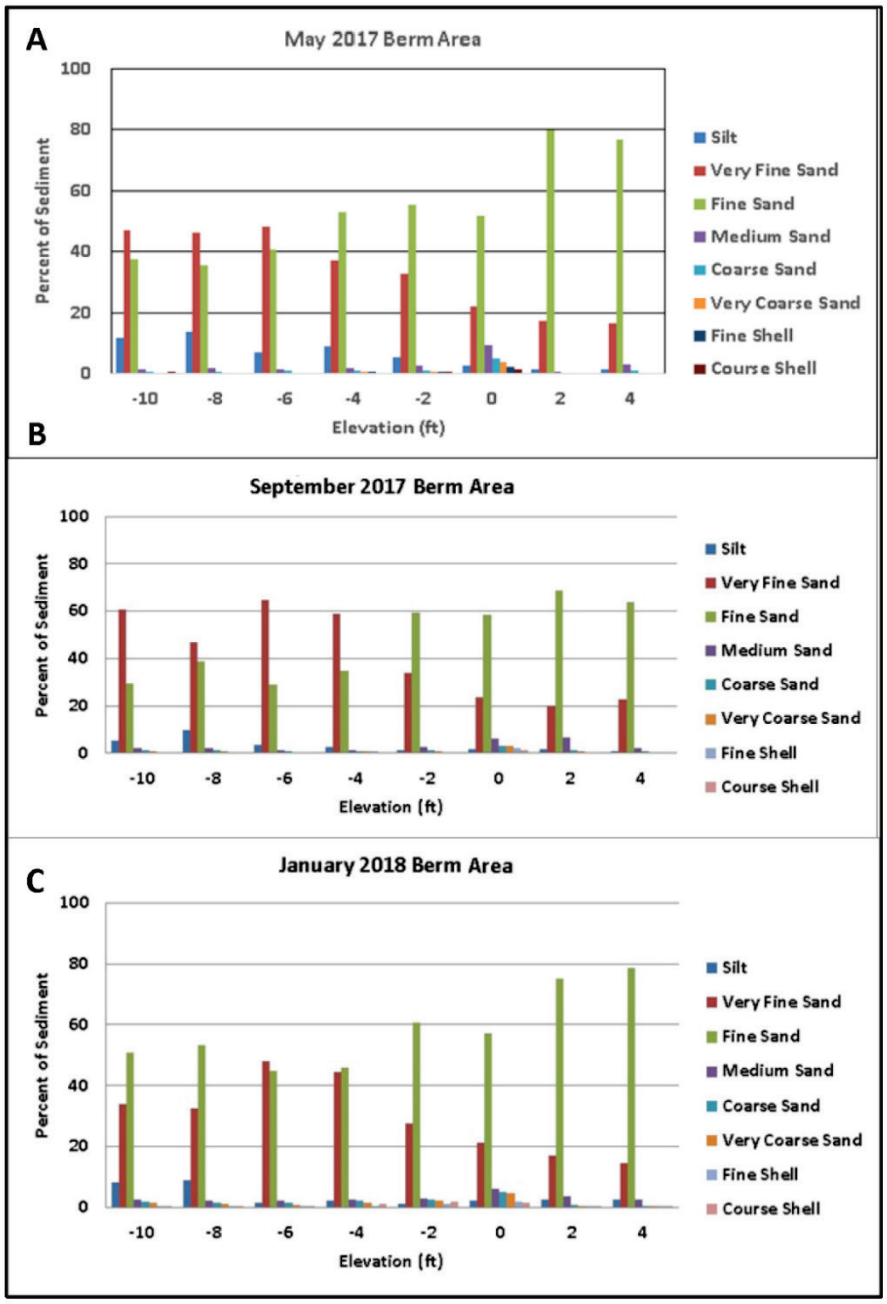

Figure 9. Average percent of sediment by size class for the south control area based on the May 2017 (A), September 2017 (B), and January 2018 (C) surveys. Silt (<0.06 mm), very fine sand (0.06–0.125 mm), fine sand (0.125–0.250 mm), medium sand (0.25–0.50 mm), coarse sand (0.50–1.0 mm), very coarse sand (1.0–2.0 mm), fine shell (2.0–4.0 mm), coarse shell (>4.0 mm) (Ramos and Zarillo 2019).

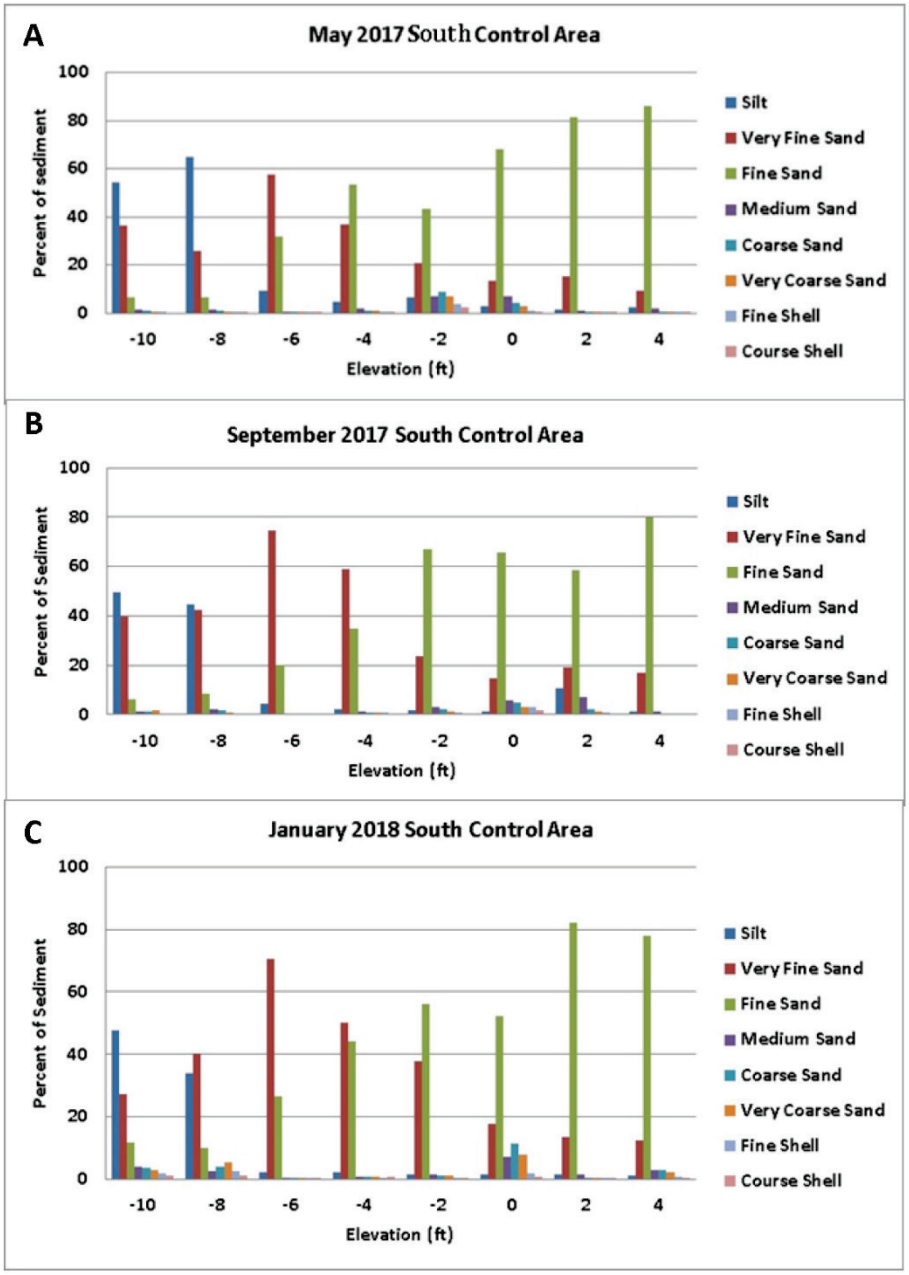

4.2 Sediment statistic test results

During the first phase of statistical analysis, Kruskal-Wallis tests determined that the differences in modal grain size among the three collection periods (May 2017, September 2017, and January 2018) were statistically significant and therefore unlikely due to chance. Further post-hoc testing was unable to identify where the differences occurred among the three groups (Figure 10). Because this test considers all sediment size collected within the study area as a single group, a large variability is expected. This is likely the cause of the inability to discern differences in the groups during the post-hoc test. Nevertheless, since the Kruskal-Wallis results indicate that there is a difference in the modal grain size among the three collection periods, more in-depth analysis was able to be conducted on each collection period separately to better discern sediment changes within the study area.

Figure 10. Modal sediment size from different collection periods. Results of the post–hoc test are shown as a letter above each group. Groups with the same letter indicate no differences between groups.

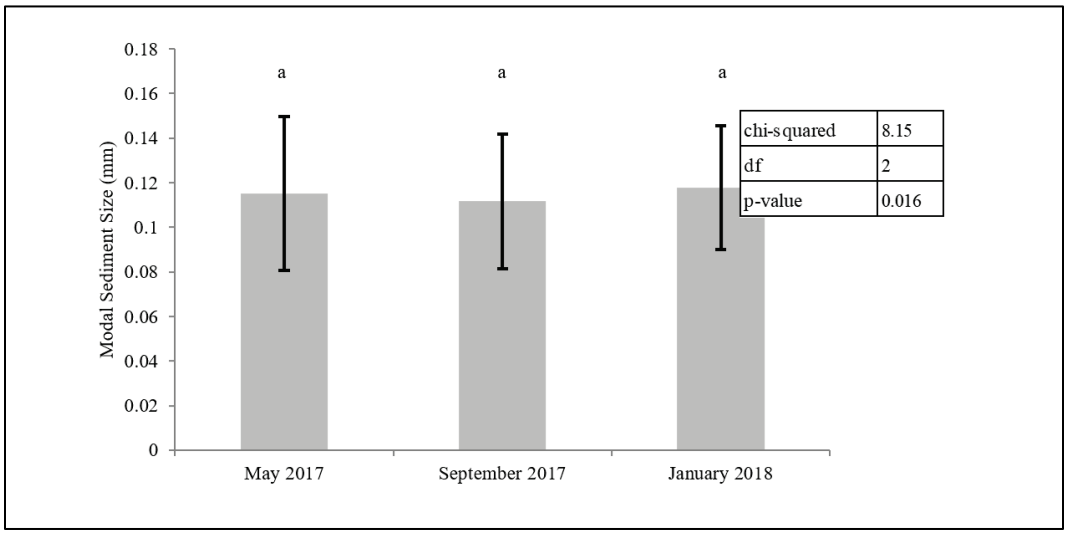

The Scheirer-Ray Hare test showed differences in modal grain size when considering area and elevation for the months of May 2017 and January 2018 (Tables 4 and 6). In September 2017, there was a difference for elevation, but there was no difference between the control areas and berm area (Table 5). Further post-hoc testing performed across areas for the three collection periods indicates that the average modal grain size within the south control area is different from the north control area during the months of May 2017 and January 2018 (Figure 11).

Table 4. Scheirer-Ray Hare results for May 2017 concerning elevation, area, and the interaction between the two. The resulting p-value for each category (Area, Elevation and Area*Elevation) is compared to an alpha value of 0.05. If the p-value is less than the alpha value, it indicates that modal sediment size differences in the given category are not due to chance and are instead statistically significant. For the May 2017 collection period, changes in sediment grain size in every category (Area, Elevation, and Area*Elevation) were statistically significant and not likely due to chance (Ramos and Zarillo 2019).

	Df	SS	F	p
Area	2	8.0E+04	12.3	0.002
Elevation	7	6.9E+05	106.8	<0.001
Area*Elevation	14	4.2E+05	64.4	<0.001
Error	314	9.9E+05		
Total	337	2.2E+06		

Table 5. Scheirer-Ray Hare results for September 2017 concerning elevation, area, and the interaction between the two. The resulting p-value for each category (Area, Elevation and Area*Elevation) is compared to an alpha value of 0.05. If the p-value is less than the alpha value, it indicates that differences in modal sediment size for the given category are not due to chance and are instead statistically significant. For the September 2017 collection period, changes in sediment grain size in Elevation and Area*Elevation were statistically significant ,whereas sediment changes in Area were similar (Ramos and Zarillo 2019).

	Df	SS	F	p
Area	2	3.9E+03	3.7	0.157
Elevation	7	6.0E+04	57.6	<0.001
Area*Elevation	14	2.7E+04	26.2	0.025
Error	103	4.0E+04		
Total	126	1.3E+05		

Table 6. Scheirer-Ray Hare results for January 2018 concerning elevation, area, and the interaction between the two. The resulting p-value for each category (Area, Elevation and Area*Elevation) is compared to an alpha value of 0.05. If the p-value is less than the alpha value, it indicates that modal sediment size differences in the given category are not due to chance and are instead statistically significant. For the January 2018 collection period, changes in sediment grain size in every category (Area, Elevation, and Area*Elevation) were statistically significant and not likely due to chance (Ramos and Zarillo 2019).

	Df	SS	F	p
Area	2	2.7E+05	46.07	<0.001
Elevation	7	4.3E+05	73.04	<0.001
Area*Elevation	14	3.6E+05	60.48	<0.001
Error	315	9.4E+05		
Total	338	2.0E+06		

Figure 11. Comparison of modal sediment sizes between collection periods grouped by location. Similarity between the groups is shown as letters, symbols, and numbers (May 2017 is shown as letters, September 2017 is shown as symbols, and January 2018 is shown as numbers). Groups with the same letter, symbol, or number indicate that changes in sediment size for the given group are likely due to chance and are therefore similar. Results show that during the May collection period, the north and berm were similar, and the berm and south were similar, but the north and south were not similar. During the September collection period, all three areas were similar. During the January collection period, the north and berm were similar, but the south was different (Ramos and Zarillo 2019).

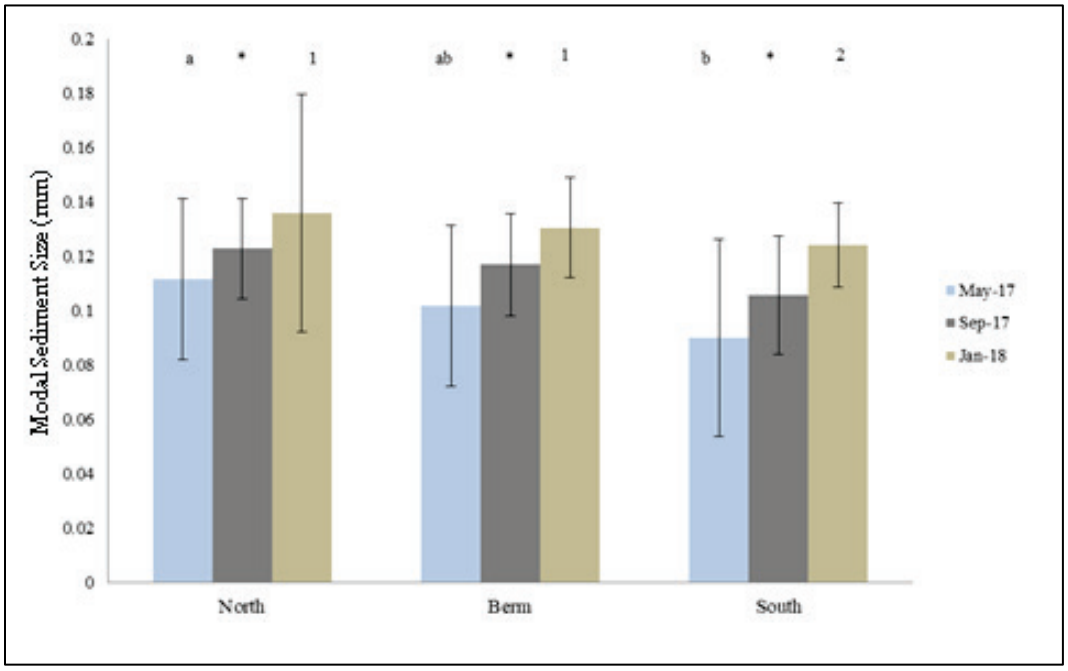

Modal sediment size distribution by elevation was statistically different for all three collection periods. Since it is well known that grain size distributions change in relation to elevation on the shoreface, this difference was expected. A further analysis comparing sediment from similar elevations is presented below in the second phase of statistical testing. Traditional post-hoc testing compares all individual elevations within the given test (e.g., a comparison of sediment from +4 ft with sediment from -10 ft). Because of the known variation of sediment size in the cross-shore direction, the average occurrence of grain size fractions is summarized by date and elevation instead of a traditional post-hoc test (Table 7).

Graphical representations of the data listed in Table 3 are shown in Figure 7 through Figure 9 . These figures along with Table 3 show that the overall percentage of very fine sand was higher in the September data at all depths. The most notable increase in very fine sand in the post storm sediment data occurred at depths of -4 to -10 ft. Changes in the relative percentages of fine sand in this period were variable across the lowered shoreface at depth of -2 to -10 ft but lower at depths of 0 ft to +4 ft. The medium to very coarse sand fraction remained low across the shoreface through sample periods along with the percentages of shells fragments. In the January sediment data set, the relative percentages of fine and very fine sand over all three areas returned to values similar to those observed in the May 2017 sediment data set.

During the second phase of statistical testing, the Kruskal-Wallis test was used to determine changes in percent of fine-grained sediment (Table 7, Table 8, Table 9) within the -2 ft and -4 ft elevations. This test determined there was a change in the percent of fine-grained <0.06 mm) material during the three collection periods (May 2017, September 2017, and January 2018). Further post-hoc testing identified a higher percent of fine-grained material within the -2 ft and -4 ft elevations during May 2017. September 2017 and January 2018 were similar in the percent of fine-grained material, which was much lower than May 2017 (Figure 12).

Figure 12. Percent fine sediment (>0.06 mm) from different collection periods. Results of the post-hoc test are shown as a letter above each group. Groups with the same letter indicate no differences between groups.

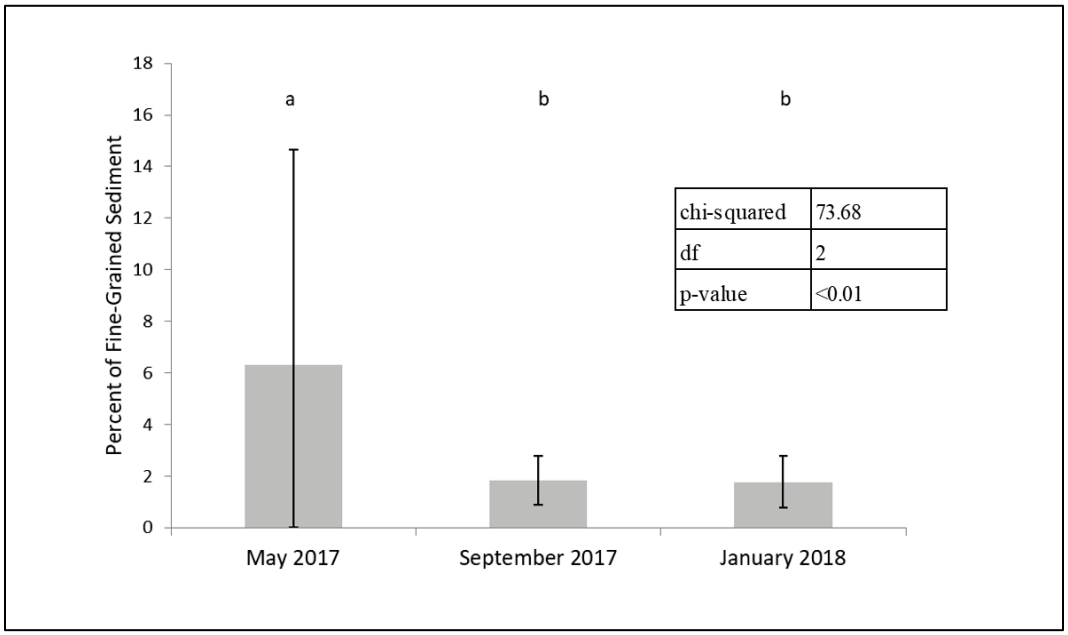

The Scheirer-Ray Hare test showed statistical differences among percentages of fine-grained sediment relative to elevation during September and January (Table 8, Table 9). In May there was no difference in the percent of fine-grained material in relation to area, elevation, or area*elevation (Table 7). Further post-hoc testing performed across areas for the three collection periods indicates that the percentage of fine-grained sediment within the -2 ft and -4 ft elevations was similar in relation to different areas (e.g., May-north contained similar percent of fine-grained material as May-berm and May-south). Visually, the Figure 13 shows a higher percent of fine-grained material during the May collections; this agrees with results from the previous Kruskal-Wallis test (Figure 12).

Table 7. Scheirer-Ray Hare results for May 2017 concerning elevation, area, and the interaction between the two. The resulting p-value for each category (Area, Elevation, and Area*Elevation) are compared to an alpha value of 0.05. If the p-value is less than the alpha value, it indicates that percent of fine-grained sediment is different in the given category and changes are not due to chance but instead statistically significant. For the May 2017 collection period, changes in percent of fine-grained sediment are similar in every category (Area, Elevation, and Area*Elevation). Therefore, any changes within these three catagories are likely due to chance.

	Df	SS	F	p
Area	2	1.9E+02	0.2	0.880
Elevation	7	1.9E+02	0.2	0.624
Area*Elevation	14	1.6E+03	1.9	0.379
Error	314	7.6E+04		
Total	337	7.8E+04		

Table 8. Scheirer-Ray Hare results for September 2017 concerning elevation, area, and the interaction between the two. The resulting p-value for each category (Area, Elevation, and Area*Elevation) are compared to an alpha value of 0.05. If the p-value is less than the alpha value, it indicates that differences in the percent of fine-grained sediment for the given category are not due to chance and are instead statistically significant. For the September 2017 collection period, changes in percent of fine-grained sediment in relation to elevation was statistically significant while changes in Area and Area*Elevation were similar. This indicates that changes in percent of fine-grained sediment in relation to elevation are likely not due to chance.

	Df	SS	F	p
Area	2	3.1E+02	3.1	0.209
Elevation	7	1.8E+03	18.0	0.012
Area*Elevation	14	4.6E+02	4.7	0.791
Error	103	7.2E+02		
Total	126	3.3E+03		

Table 9. Scheirer-Ray Hare results for January 2018 concerning elevation, area, and the interaction between the two. The resulting p-value for each category (Area, Elevation, and Area*Elevation) are compared to an alpha value of 0.05. If the p-value is less than the alpha value, it indicates that differences in the percent of fine-grained sediment within a given category are not due to chance and are instead statistically significant. For the January 2018 collection period, changes in percent of fine-grained sediment in relation to elevation was statistically significant while changes in Area and Area*Elevation were similar. This indicates that changes in percent of fine-grained sediment in relation to elevation are likely not due to chance.

	Df	SS	F	p
Area	2	3.7E+02	0.46	0.795
Elevation	7	6.8E+03	8.43	0.038
Area*Elevation	14	3.9E+03	4.80	0.187
Error	315	6.7E+04		
Total	338	7.8E+04		

Figure 13. Comparison of percent of fine-grained material within -2 ft and -4 ft elevations in relation to collection periods grouped by location. Similarity between the groups is shown as letters, symbols, and numbers (May 2017 is shown as letters, September 2017 is shown as symbols, and January 2018 is shown as numbers). Groups with the same letter, symbol, or number indicate that changes in sediment size for the given group are likely due to chance and are therefore similar. Results show that when considering collection periods individually, all three areas (north, berm, south) contained a similar percent of fine-grained sediment within the -2 ft to -4 ft depth range

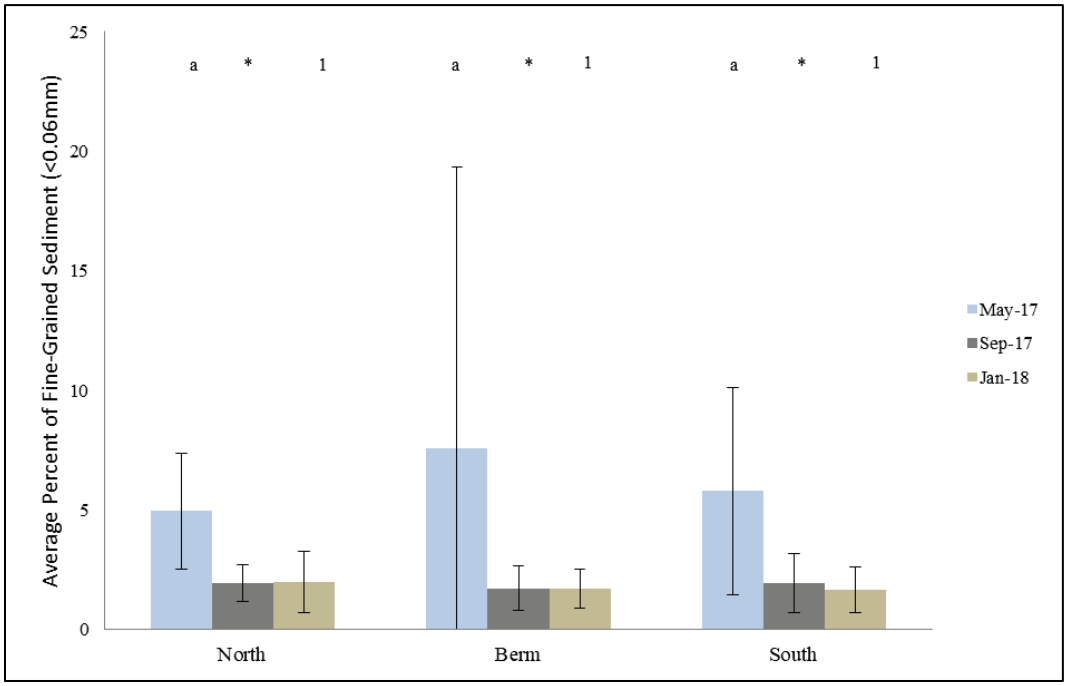

4.3 Carbonate distribution

The carbonate content of sediments in the project area was examined to determine the importance of carbonate-rich sediment sources in the project area the study area. The carbonate is predominantly from shell fragments distributed across all sediment grain-size fractions along a high percentage of carbonate content in the silt sediment fraction. Visible shell fragments appeared to be weathered fossil material and may be derived from erosion of the underlying carbonate lithology. Geographic plots of carbonate percent allow inference as to the source of carbonate material.

All three sample collection periods had a high percent of carbonate material in the south control area, parts of the swash zone, and offshore at the base of the shoreface in all areas. Very little carbonate material occurred in sediments of the upper shoreface within the berm area (Figure 14). The carbonate fraction mixing with terrigenous appeared to be weathered fossil material and may be derived from erosion of the underlying lithology carbonate-rich shelly sediments of Tertiary to early Quaternary age termed TQsu on the Florida Geological Map (Figure 2). The depth of these carbonate-rich units below Holocene sands of the Fort Myers Beach area is unknown but may be within reach of surface erosion during storms. Higher percentages of carbonate found in samples in depths of -10 ft at the base of the shoreface are consistent with the fact that modern barrier islands of Florida are relatively thin wave-built deposits resting on older carbonate platforms. Beyond the shoreface, the continental shelf of the west Florida coast is dominated by exposed limestone formations and isolated sand deposits (USGS 2001).

Figure 14. Carbonate percentages in the May 2017 (A), September2017 (B), and January 2018 (C) sediment samples. Warmer colors indicate larger percentage of carbonate material.

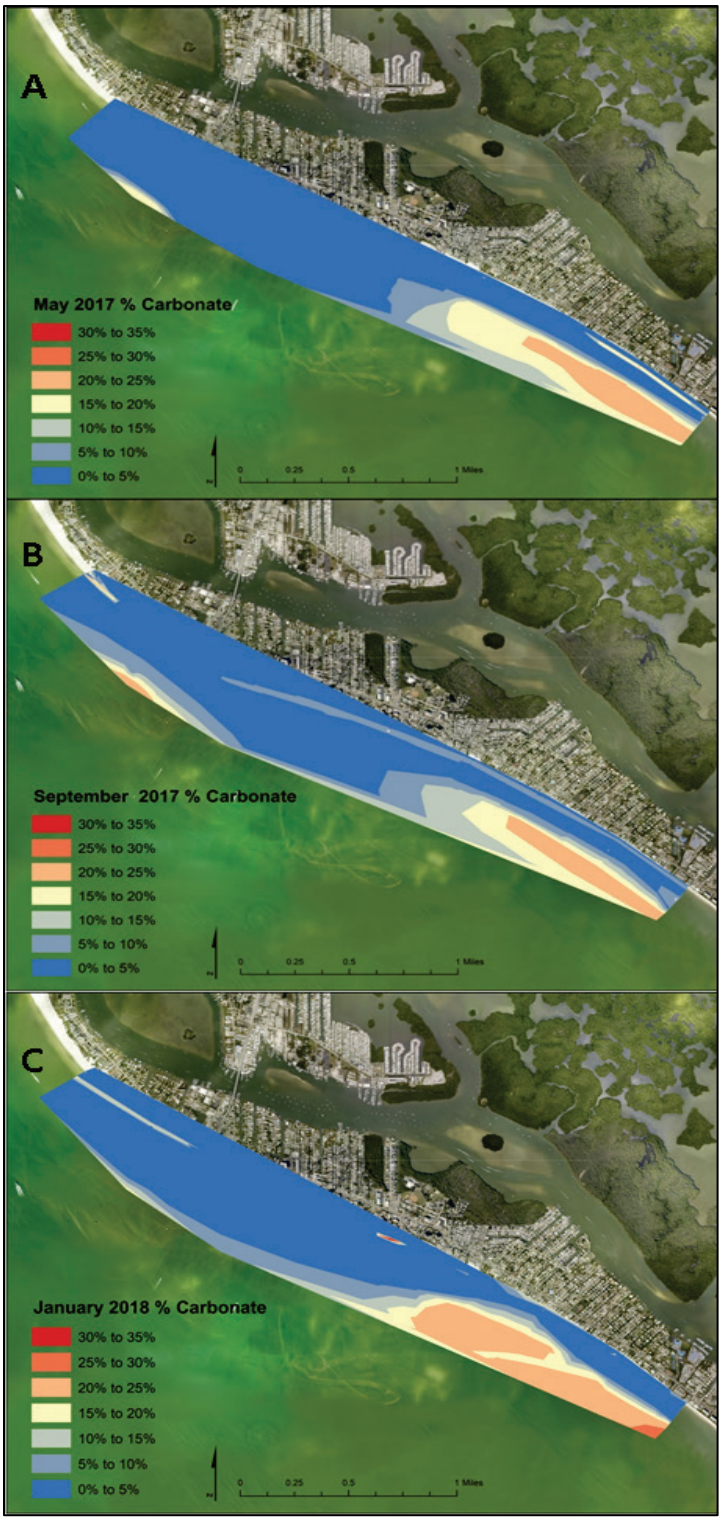

4.4 Suspended sediment concentrations

The primary contributing factors to high suspended sediment concentrations are wave and current action along with finer sediment fractions available for suspension in the water column. Suspended sediment concentrations can also vary based on date, time, collection method, and other site conditions that may prevail at the time of collection. As described under Section 3 (Methods), suspended sediment samples were collected over several days using two collection methods. Therefore, directly comparing water column sediment concentrations has limitations. In May 2017, most of the -2 and -4 ft suspended load samples were collected from the beach on Monday May 23. Further collection was then delayed until Wednesday May 24 due to adverse weather conditions. In January 2018, suspended sediment samples were collected in single day under moderate conditions consisting of 30 cm waves at a period of approximately 6 sec.

Figure 15 presents vertically averaged suspended sediment concentrations by profile location over -2 ft, -4 ft, and -8ft cross-shore bathymetric locations. The values shown in Figure 15 and in Table 10 and Table 11 are the average of the near- surface, mid-depth, and near-bottom sample concentrations. Extreme concentrations values of more than 2,000 mg/l were eliminated in an attempt to mitigate the errors introduced by the sampling methods such as turbulence caused by sampling personal and near bottom turbulence caused by sampling bottles in the lower part of the benthic boundary layer. The alongshore extend of the berm area is shown in Figure 15.

There are no distinctive visual patterns within the suspended sediment plots that are related to the berm location. However, as listed in Table 10, the spatially averaged concentrations are highest over the nearshore -2 ft depth contour and lowest over the -8 ft contour. Further, water column concentrations at all locations are higher in the January 2018 data set compared to the May 2017 data set. Table 11 lists the spatially average suspended sediment concentrations over each bathymetric location for the north control area, berm area, and south control area. Sediment concentrations were higher in the berm area compared to the north and south areas for all depth locations during each sampling event except over the -2 ft bathymetric contour in the January 2018 sample set (Table 11).

Figure 15. Depth-averaged suspended sediment concentrations from the May 2017 and January 208 sampling periods. Concentrations are based on averaging the surface, mid-depth, and near-bottom values. Panel A: concentrations: over the -2 ft depth contour. Panel B: concentration over the -4 ft contour. Panel C: concentration over the -8 ft. contour. Profile names are listed from north to south along the X-axis.

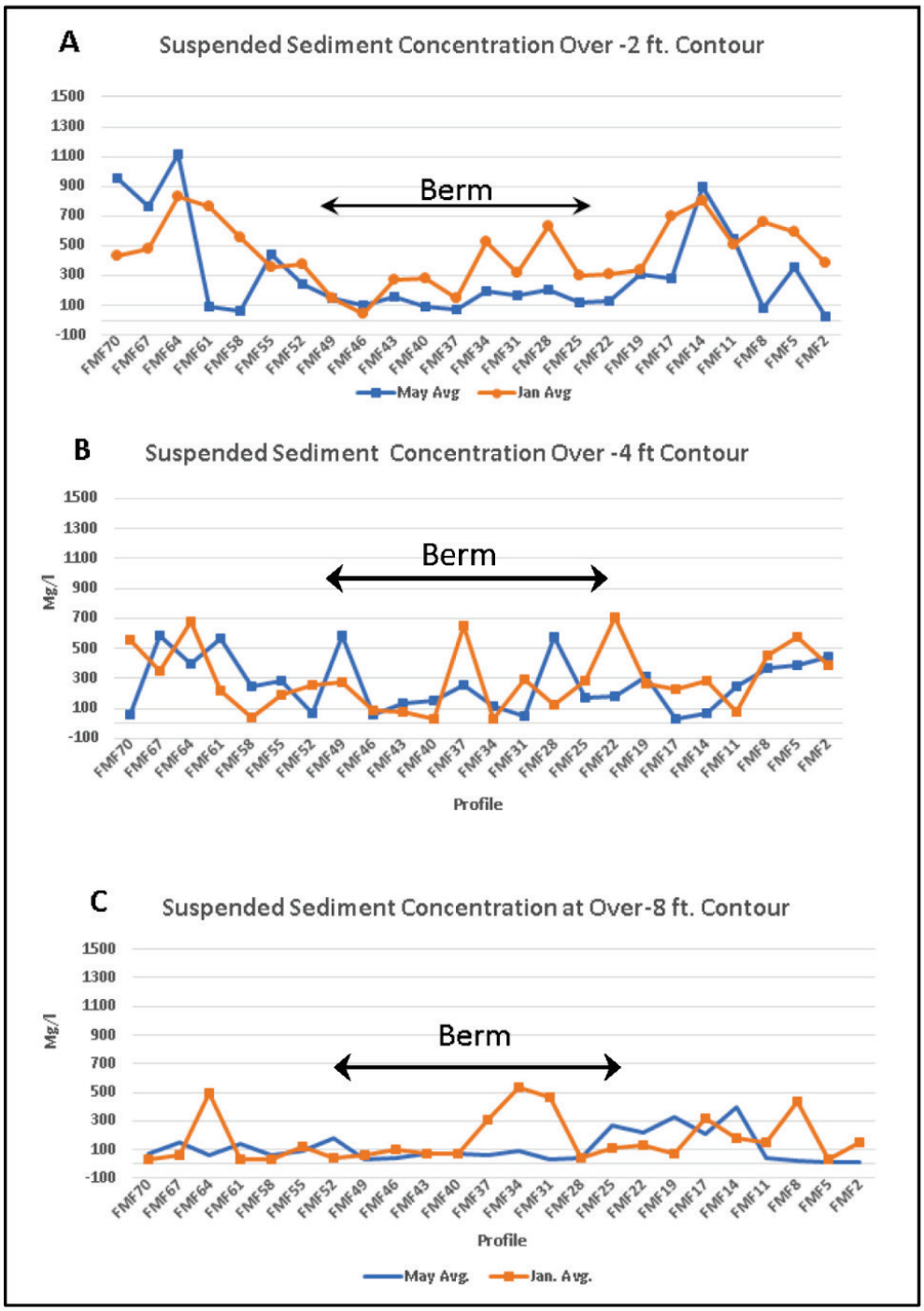

Table 10. Average suspended sediment concentrations by depth contour in units of milligrams/liter.

Location	May 2017	January 2018
-2 ft Contour	341	445
-4 ft contour	262	318
-8 ft Contour	121	179

Table 11. Suspended sediment concentrations by depth contour and by area in units of milligrams/liter.

Location	May 2017	January 2018
-2 ft North Area	119	401
-2 ft Berm Area	136	296
-2 ft South Area	61	570
-4 ft North Area	60	81
-4 ft Berm Area	228	221
-4 ft South Area	37	62
-8 ft North Area	29	19
-8 ft Berm Area	77	207
-8 ft South Area	63	21

Higher suspended sediment concentrations at shallower depths are consistent with turbulence expected in this area of shoaling and breaking waves. The higher suspended sediment concentrations measured in the berm area could be linked to higher percentages of silt found in this area in the September 2017 and January 2018 sample data set compared to the north area. In the January suspended sediment data, concentrations were higher over the -2 ft contour in the south control area where percentages of silt in surficial sediments were persistently higher over all three sampling periods.

A regression analysis was conducted to detect correlation between surface, mid-depth, and bottom sediment concentrations with respect to underlying sediment indices. No strong correlation was found between bottom sediment attributes and suspended concentrations. Possible correlations were examined with respect to bottom sediment mean grain, model grain size, percent fine fraction, and skewness of bottom sediment grain size distribution. It is likely that that variation in wave energy is among the most important factors controlling suspended sediment loads at any point in time However, the correspondence of

higher vertically averaged suspended sediment concentrations with the berm area, along with higher concentrations at the -2 ft. contour in the silt-rich south area, indicate a possible influence of bottom sediment.

4.5 Summary of sediment data

Directly after Hurricane Irma, a general fining of sediment size on the lower shoreface was observed in the September 2017 data set marked by a distinct increase in the very fine sand fraction. Overall, the relative abundance of sediment size classes returned to pre-storm conditions. There were distinct differences among the north, berm, and south control areas with respect to sediment distribution and reaction to storm conditions. Among the three areas, the south control area is most distinctive with respect to the silt fraction, which occurred in persistently high percentages in all sampling periods. The imprint of Hurricane Irma on sediment distribution in the South control areas was an increase in the abundance of the very fine sand fraction at the expense of the fine sand and silt fractions. In the January 2018 sediment data set, the very fine sand remained high and did not return to the pre-storm distribution. The dominating sediment at depths of -4 ft to -8 ft remained between very fine sand and silt. The very fine sand fraction in the south area also noticeably increased by January 2018 at the -2 ft sample location compared to the earlier sample results indicating possible onshore moment of this fraction in the post storm period. Another possible source of this size fraction was southward movement of very find sand from the berm and north control area, which experienced a particularly notable decline in very fine sand at depths between -4 ft and -10 ft from September 2017 to January 2018.

The north control area and berm area responded similarly to the storm with respect to the very fine and find sand fractions consisting of increases in very fine sand and correspond with a decline in the fine sand fraction at depths of -4 ft and greater. However, the silt content declined in the Berm area between May2017 and September 2017 whereas the silt content increased in the north control area. Overall, there is balance between the most abundant very fine sand and fine sand classes that consist of cross-shore and alongshore movement depending on energy level. The inverse abundance relationship of silt content in the north control area and berm area seen in Figure 7 and Figure 8 may indicate alongshore exchange of fine sediments dependent on energy conditions in which noticeable losses of silt across the berm

area corresponded to a significant gain in the silt fraction in the north central areas at the -10 ft sample location. The persistent high silt content in the south control area may be due to combination of a local source from erosion of underlying sediments, as well as exchanges across the berm area.

The control and berm areas were statistically similar with respect to modal grain size. This indicates a mixing caused by the hurricane. After the hurricane, sediment distributions returned to pre-storm conditions with the exception of overall silt content, which remained low compared to values observed in the May 2017 data set. Thus, the signature of storm-induced changes in sediment grain size distribution is largely recorded in the abundant finer sediments compared with the less abundant coarser size fractions. A consequence of the of Hurricane Irma on shoreface sediments storm is the onshore shift of the sediment mixing zone closer to the shoreline compared with pre-storm sediment texture.

The south control area was statistically different from the north control area in terms of grain size during the months of May 2017 and January 2017. Analysis of carbonate sediment shows that the south control a contains a higher percent of carbonate than the rest of the study area over the three collection periods. The persistent higher carbonate content in the south control area is likely a result of exposure of the underlying geological formations. As previously discussed, the Fort Thompson Formation and Tamiami Formation are located near the study area and contain a higher percentage of fine sediments and fossil material than the overlying Holocene sediments. It is likely that these formations are intermittently exposed in the south control area and contribute finer sediments and carbonate material to the littoral sediment.

Suspended sediment concentrations showed spatial and temporal variability that is logical with respect to energy level and with respect to depth and the impacts of a passing storm. Average suspended sediment concentrations on the upper shoreface were found to be higher than concentrations on the lower shoreface in both the May 2017 and January 2018 sample data sets. The average suspended sediment concentrations were higher than the January 2018 data set. The average suspended sediment concentrations at almost all sample locations in

the berm area were higher compared to the north and south control areas.

4.6 Morphological evolution

Nearshore berm morphological changes occur on short- and long-term time scales. Both types of changes must be quantified to understand the evolution and impact of the nearshore berm. In this study, consideration is given to movement of morphological features and shoreline changes. A combined analysis including changes to profiles, elevation, and volume allows for a better understanding of the morphologic evolution of the project area.

4.6.1 Cross-shore profile analyses

Analysis of cross-shore morphology was conducted on a total nine transects including three representative transects in each control area and three in the berm area (Figure 37–Figure 42).

The south control area is best represented by transect 3 shown in Figure 16 and is located approximately 1.4 mi southeast of the nearshore berm. Overall, the profile shape indicates sand volume loss from the supratidal beach and shallow part of the upper shoreface along with a corresponding deposition of sediment below the mean lower low water elevation. The two most active areas are observed in the trough between the natural sand bar and the upper shoreface and offshore. The trough gradually deepens during winter months and fills in during summer months. Winter months show a general deepening of less than 1 ft whereas summer months show an accumulation of slightly over 1 ft. The offshore section beyond 500 m shows sand accumulation in September 2017 and January 2018 of approximately 2 ft. This is likely due to a combination movement of sand from the beach and upper shoreface to offshore areas during Hurricane Irma (Figure 16) as well as southward movement of sand though the project area as described under the sand budget description in this report (see Section 4.7).

Figure 16. Profiles for all collection periods of transect FMB3 located in the south control area.

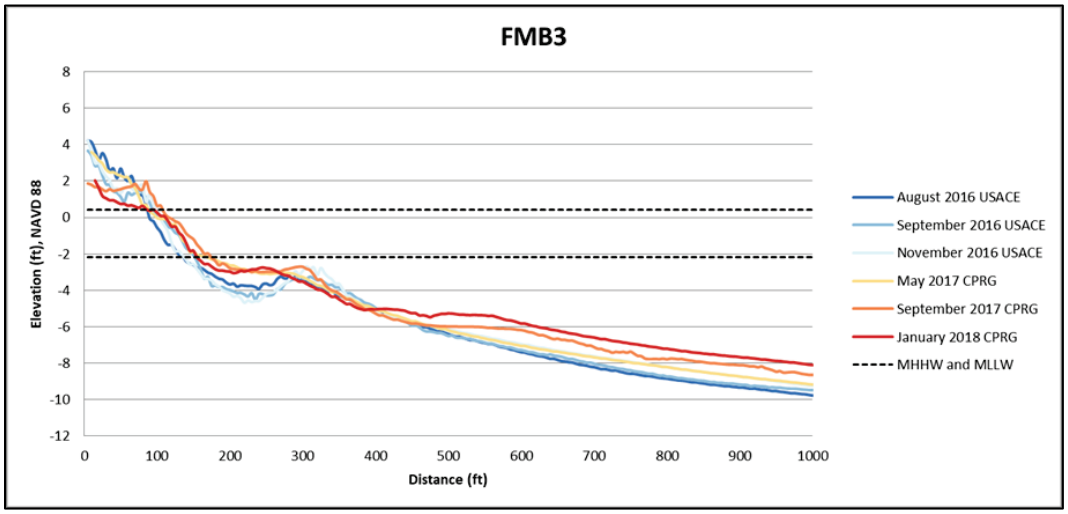

The nearshore berm area (represented by FMB46) shows substantial mobility between the months of August 2016 and November 2016 (Figure 17). This mobility includes onshore movement of the nearshore berm as well as a general reduction in berm height. When originally deposited, the berm crest was located at approximately 625 ft offshore. Within 4 months after placement, the berm crest migrated shoreward approximately 125 ft and decreased approximately 0.5 ft in elevation. From May 2017 to September 2017, the nearshore berm continued to decrease in height as the shoreface showed accretion near the swash zone. An increase in storm events during the month of January 2018 eroded some of the accretion within the swash zone and deposited it offshore. Overall, there the beach width increased as the shoreline position underwent a net seaward advance even with the influence of Hurricane Irma in September 2017. This indicates that the nearshore berm likely protected the dry beach area during the hurricane and large winter storm events (Figure 17). The corresponding change in the shoreline position with respect to the berm location and the occurrence of Hurricane Irma is discussed in a later section of this report.

Figure 17. Profiles for all collection periods of transect FMB46 located in the berm area.

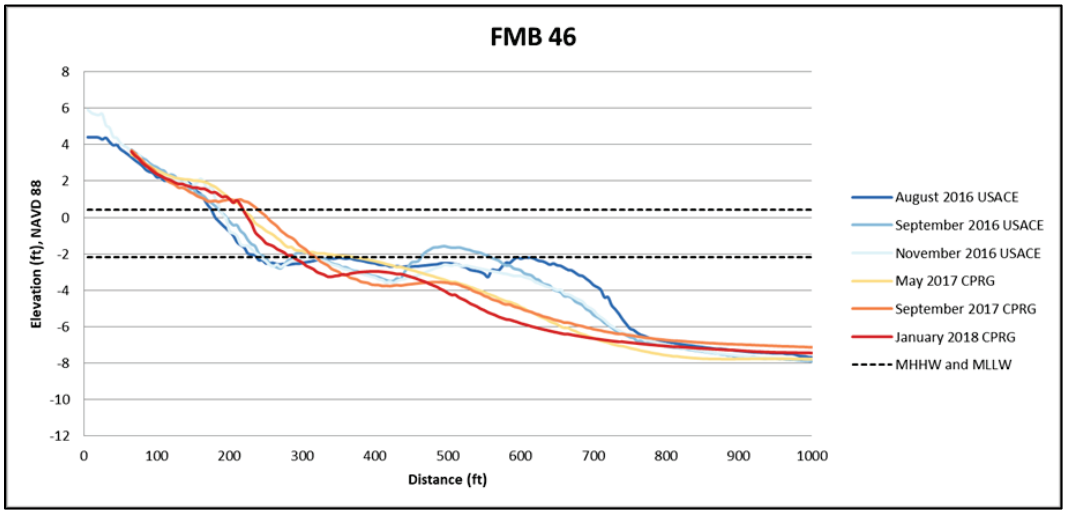

The north control area is represented by FMB56 (Figure 18), which is located approximately 1.2 mi north of the berm. This area is similar to the South control area because there was limited variation throughout the study period. Variations in this profile are likely associated with seasonal changes. There is a general decrease in elevation on the dry beach and the natural offshore bar from August 2016 to January 2018 (Figure 18).

Figure 18. Profiles for all collection periods of transect FMB56 located in the north control area.

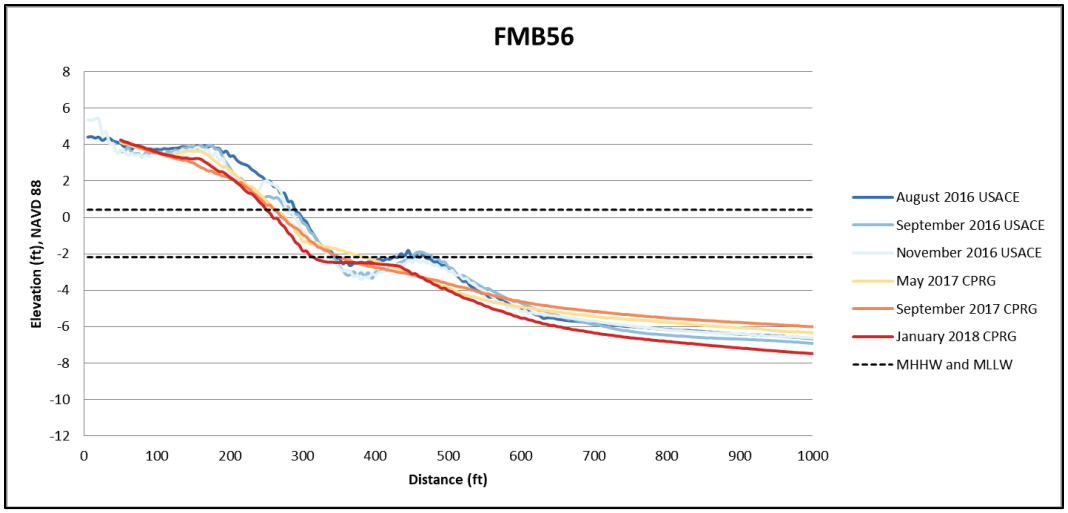

Alongshore spatial averaging of profiles over time for each area was preformed to determine overall morphology in study area. Figure 19 shows the natural bar features in the north and south control areas at approximately 300 ft from the beginning of the profile line and a larger nearshore berm feature within the berm area approximately 500 ft from beginning of the profile. The south control area is also approximately 1–2 ft lower than either the north control or berm areas. This is likely influenced by the topography of the underlying geological formation. As discussed earlier, a veneer of sand covers the underlying formations, and therefore topography of these formations is likely to influence the surface elevation.

Figure 19. Average of all profiles within each area (north control area, nearshore berm area, and south control area) for all time periods.

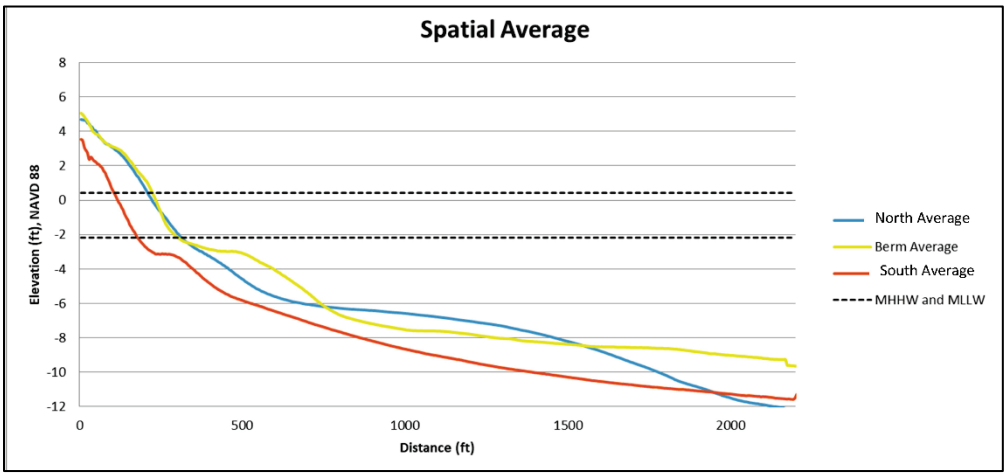

4.6.2 Topographic surface analysis

Profile analyses provides some insight on cross-shore sediment movement, but it does not provide insight on alongshore sediment movement. Alongshore sediment movement and the local sand budget are addressed in a later section of this report.

From August 2016 to September 2016, approximately 1 to 1.5 ft of erosion occurred near the top center of the Berm whereas parts of the beach and upper shoreface showed a sediment gain of approximately 1 to 3.5 ft. Figure 20 shows the change in elevation approximately 2 months after placement of the berm. The dominant net topographic changes in the north and south control areas were patches of deposition on the upper shoreface of 1 to 1.5 ft. (Figure 20).

Figure 20. Elevation changes between August 2016 and September 2016. Warmer colors indicate accretion, and cooler colors indicate erosion.

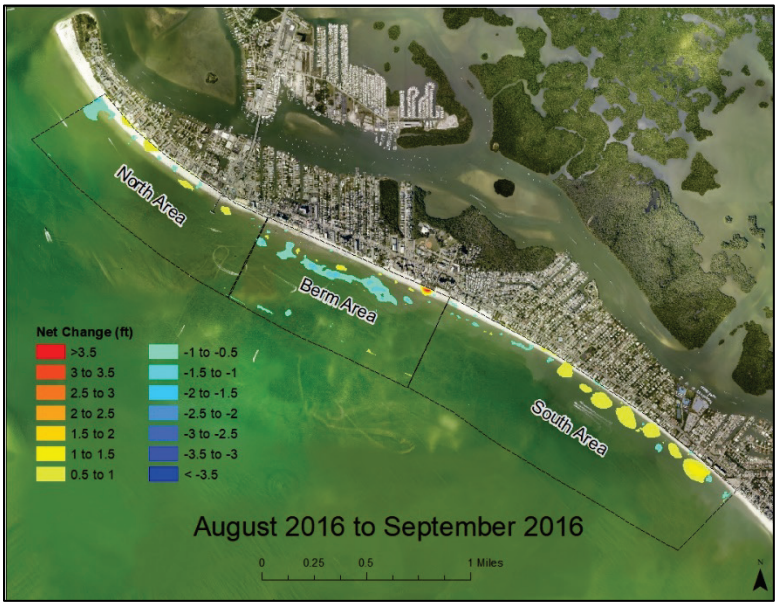

From September 2016 to November 2016, very little change occurred throughout the study area. The small section of beach that showed sand accumulation continued to increase in height by approximately 1 to 2 ft (Figure 21). Net topographic changes in the north and south control areas consisted of a patchwork of primarily 0.5 to 1.0 ft of erosion on the upper shoreface and clusters of deposition on the mid to lower shoreface in the berm area.

Figure 21. Elevation changes between September 2016 and November 2016. Warmer colors indicate accretion, and cooler colors indicate erosion.

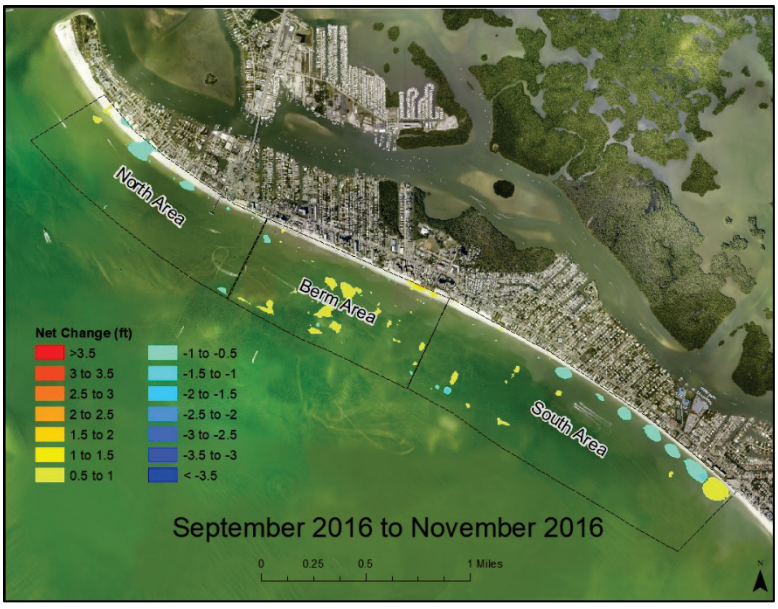

The approximate 6-month period between the November 2016 survey and the first topographic survey conducted by the CPRG for this project in May 2017 was more topographically active compared to topographic differences over the shorter September to November 2016 survey period (Figure 22). Topographic changes on the berm area are consistent with the representative profile shown in Figure 17. Berm sediments continued to move onshore to the upper shoreface where elevations increased by approximately 1 to 3 ft along with corresponding erosion and topographic decrease in the original berm construction area. The lower shoreface of the berm area was characterized by alternating zones of 1 ft of deposition and erosion. The north control area included a large mid- to upper shoreface zone of slight erosion and smaller zones of deposition on the beach.

The south control area included a nearly continuous zone of deposition on the upper shoreface at the north end, followed by a broad zone of deposition on the mid to lower shoreface in the mid-section of the area. The south section was dominantly erosion on the upper shoreface along with smaller zones of deposition. A narrow zone of erosion reaching 1 ft of change or less is seen at the south end of this zone (Figure 22).

Figure 22. Sand volume changes between November 2016 and May 2017. Warmer colors indicate accretion, and cooler colors indicate erosion.

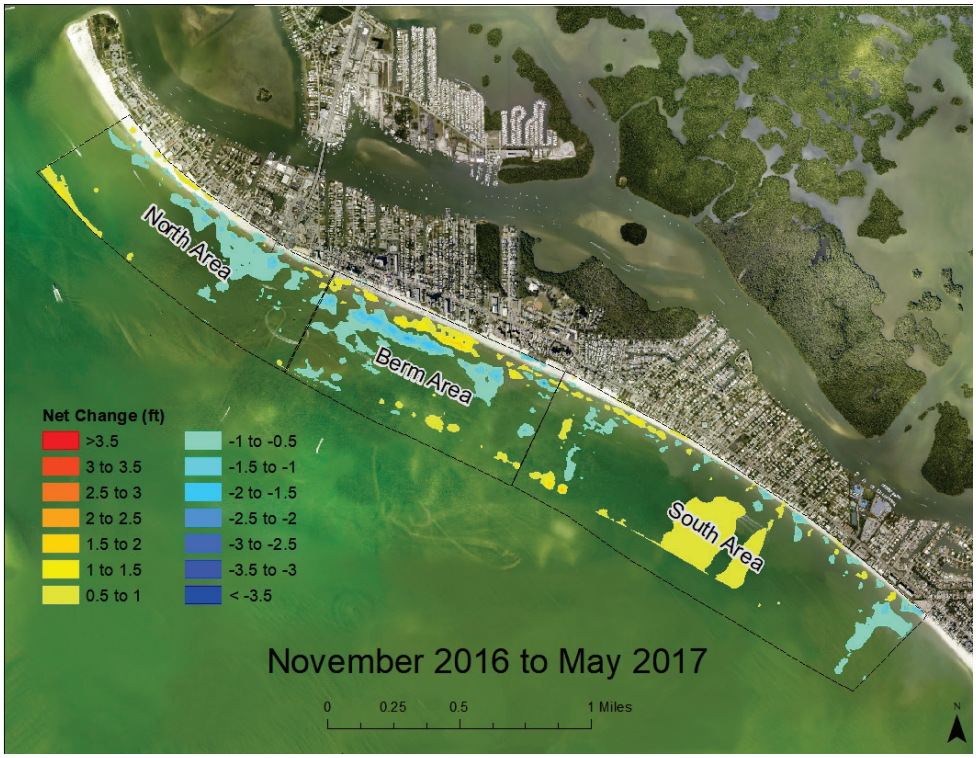

The May 2017 to September 2017 period includes topographic changes influenced by Hurricane Irma (Figure 23) The north control area is characterized by some erosion on the upper shoreface and a section of the beach along with a broad area of deposition on the mid to lower shoreface. This pattern carries over into the north section of the berm area, along with zones of deposition on the upper shoreface as berm sediments continued to move onshore. A zone from the middle of the berm area to the middle of the south control area includes erosion of approximately 0.5 to 2 ft across the mid to lower shoreface and zones of deposition on the upper shoreface. The southernmost section of the south control area includes a broad zone of deposition across the upper to lower shoreface of approximately 0.5 to 1.5 ft (Figure 23).

Figure 23. Elevation changes between May 2017 and September 2017. Warmer colors indicate accretion, and cooler colors indicate erosion.

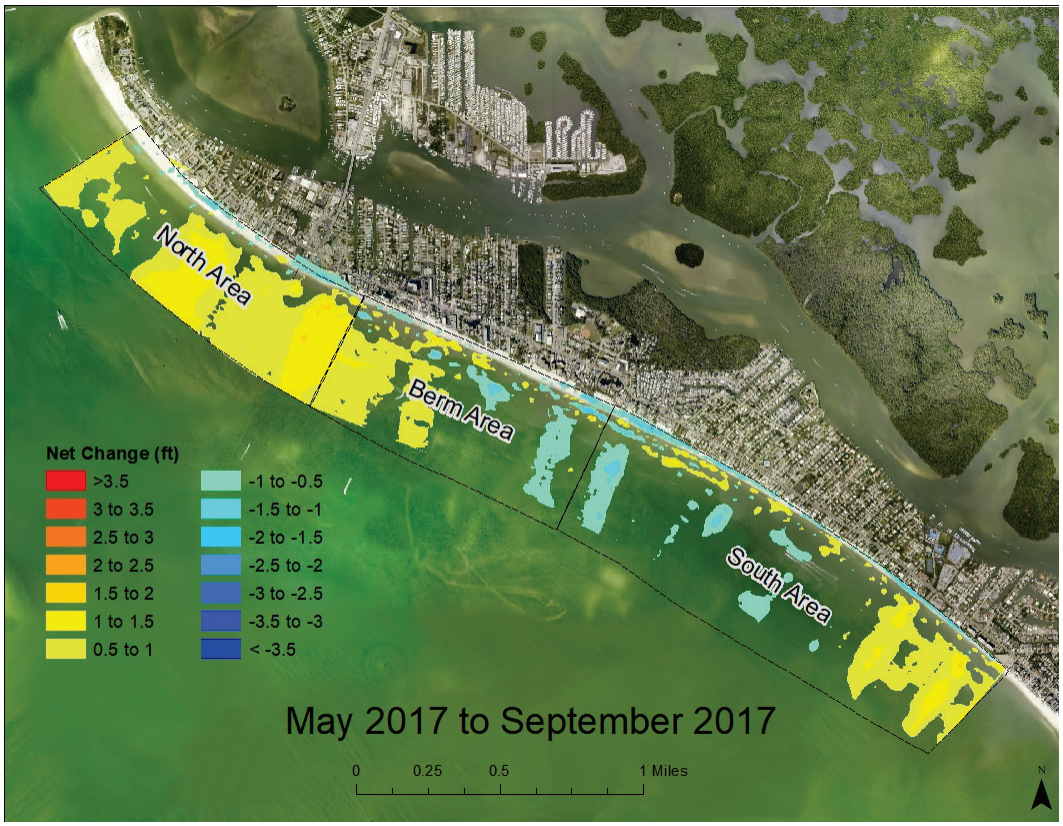

From September 2017 to January 2018, the pattern of topographic change was largely the reverse of the May 2017 to September 2017 pattern. Erosion of the mid to lower shoreface and deposition on the upper shoreface occurred along with zones of deposition on the beach. Deposition zones on the upper shoreface and beach are particularly

apparent on in the berm area (Figure 24). Some areas of beach also experienced accumulation that may be associated with the emergency nourishment project directly after Hurricane Irma. The pattern from September to January 2018 is consistent with an erosion and recovery pattern that may be associated with the passing of Hurricane Irma. Sedimentologically, the post storm recovery is associated with overall average increases in fine sand percentages at most depths and a corresponding decrease in very fine sand in all three areas. The only noticeable change in the silt size fraction was in the north control area where the fine-grained fraction declined by approximately 10% at the base of the shoreface.

Figure 24. Elevation changes between September 2017 and January 2018. This period includes the effects of Hurricane Irma. Warmer colors indicate accretion, and cooler colors indicate erosion.

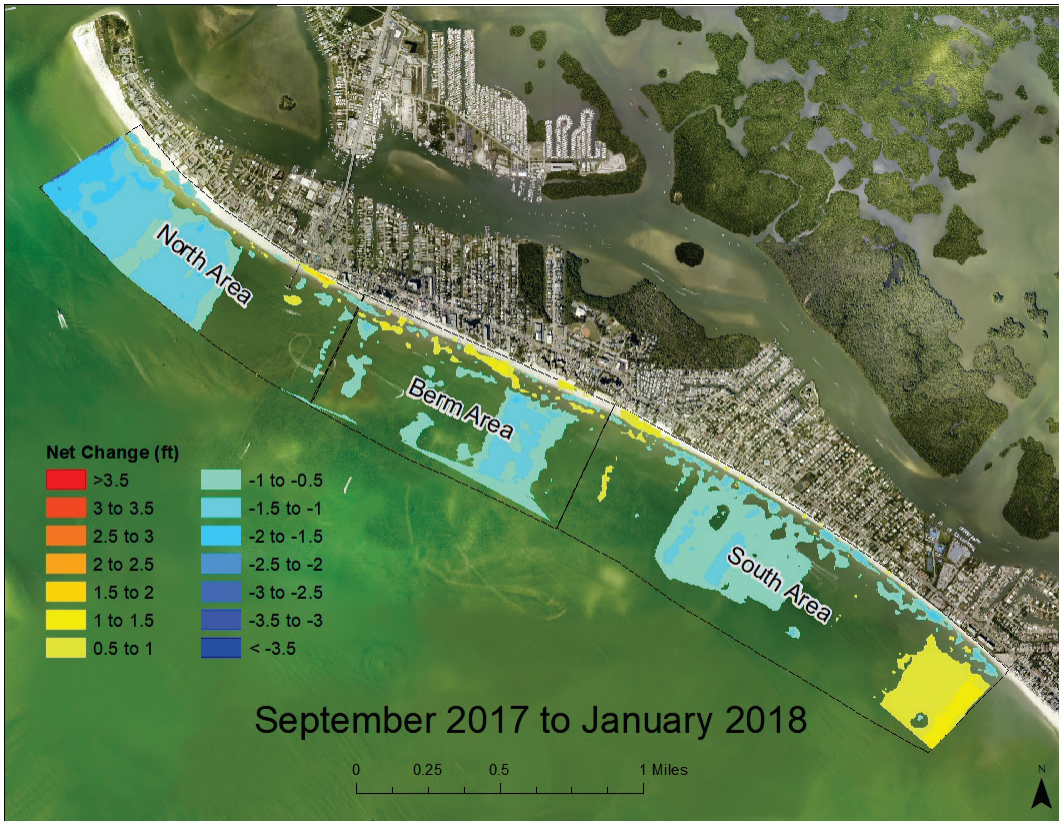

The overall pattern from the first survey to final topographic survey of this study (August 2016–January 2018) is likely the combination of equilibration of the berm to the local physical environment, a response to the passing of Hurricane Irma, and possibly net southward movement of sediment into the south control area. In Figure 25,

onshore migration of berm sediments is very apparent and marked by up to 4 ft of erosion over the original berm location and 2 ft and more of deposition on the upper shoreface and beach. This interpretation of the berm is also manifested in the profile analysis (Figure 17) as well as in the shoreline analysis presented later in this report.

Large sections of the north and south control areas have similar erosion patterns, but mid to lower shoreface erosion is not combined with upper shoreface and beach deposition. A prominent zone of deposition over the mid to lower shoreface occurs within the southern third of the south control area in combination with erosion of the upper shoreface and beach. This zone was also present in the May 2017 to September 2017 (post-storm) topographic comparisons as well as in the September 2017 to January 2018 comparisons.

Figure 25. Elevation changes between entire study period (August 2016 to January 2018). Warmer colors indicate accretion, and cooler colors indicate erosion.

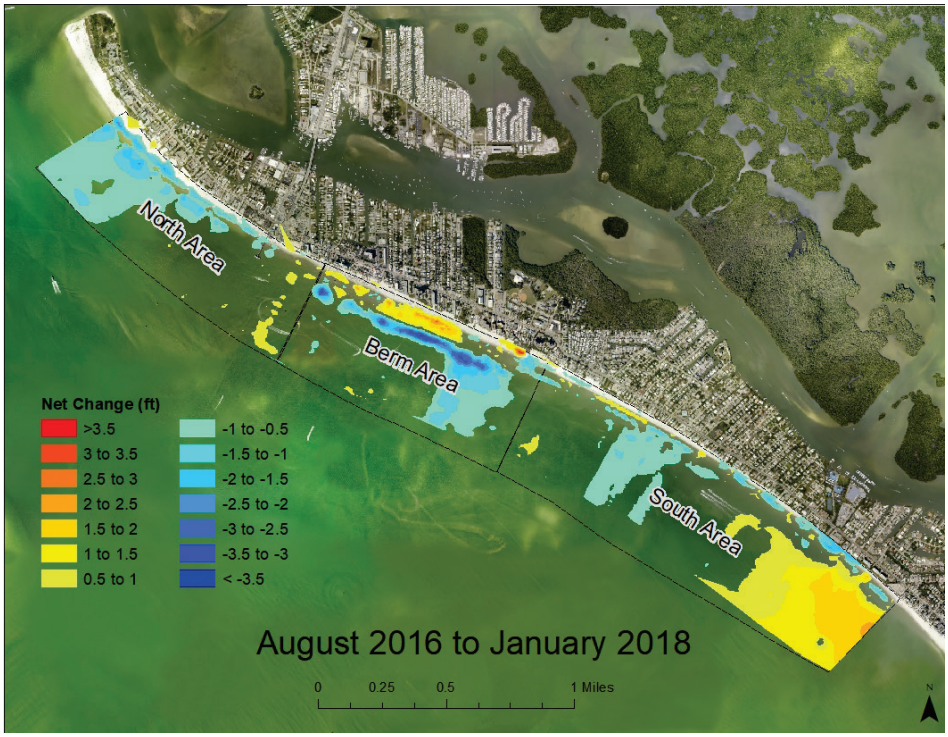

4.7 Analyses of volume changes and local sediment budget

Differences in volume changes between surveys are based on calculations relative to a fixed base-elevation. Fluctuation of sediment volumes in the berm and control areas is consistent with measured topographic and profile data. Figure 26 shows volume changes between

survey dates in the berm and control areas. The two clusters on the right-hand side of the bar plot show the net sediment volume changes between August 2016 and January 2018 and between September 2016 and January 2018, respectively. Net volumetric changes over these longer time periods provide insight on constructing a sediment budget for the study area in terms of source of sand volume to initialize budget. Note that among all of the surveys, the south control area gained sand volume in all periods except the post storm interval from September 2017 to January 207. The net volume gain in the south area was close to 200,000 yd^3 over the approximate 17-month period between August 2016 and January 2018. Three alternative sediment budgets were calculated using these net volume changes to characterize sediment movement over the project time period.

Figure 26. Changes in sand volume in relation to collection period.

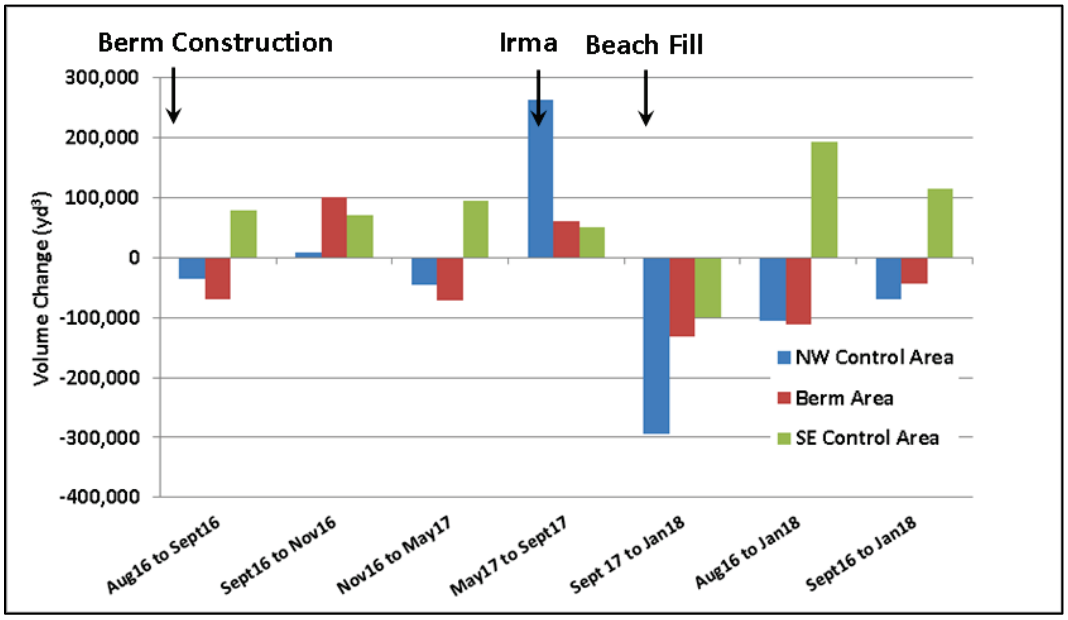

A large sand volume gain in the north control area was observed between the May 2017 topographic survey and the post-storm survey of September 2017. This area of sediment volume gain can be seen in Figure 23 showing net topographic changes for this period of time. Smaller volume gains were observed in the berm and south control areas in this period (Figure 26). The magnitude of the storm surge disturbance relative to normal and precited waters levels at the Fort Myers NOAA/National Ocean Service Station 8725530 is shown in Figure 27, which plots water levels for the month of September 2017. The total range of water levels changes from lowest to highest levels was

approximately 6 ft. Potentially, the surge-related water level fluctuations created a large hydraulic gradient between the interior of the coast and the coastal ocean driving extreme currents that mobilized sediments. The normal, largely mixed diurnal tide was overwhelmed by the effects of the storm surge for approximately 2 days, as seen in Figure 27.

The final project topographic survey in January 2018 revealed that the large volume sediment accumulated in the project area period from May 2017 to September 2017 was dispersed as seen by the reduction in sand volume between September 2017 and January 2018. As noted in Section 4.2, volumetric and topographic changes related to Hurricane Irma also corresponded to noticeable sediment changes in the relative abundance of finer size fractions in which fine sand percentages increased relative to the very fine sand fraction.

Figure 27. Observed and predicted water levels at the Ft. Myers NOAA Station 8725530 for the month of September 2017.

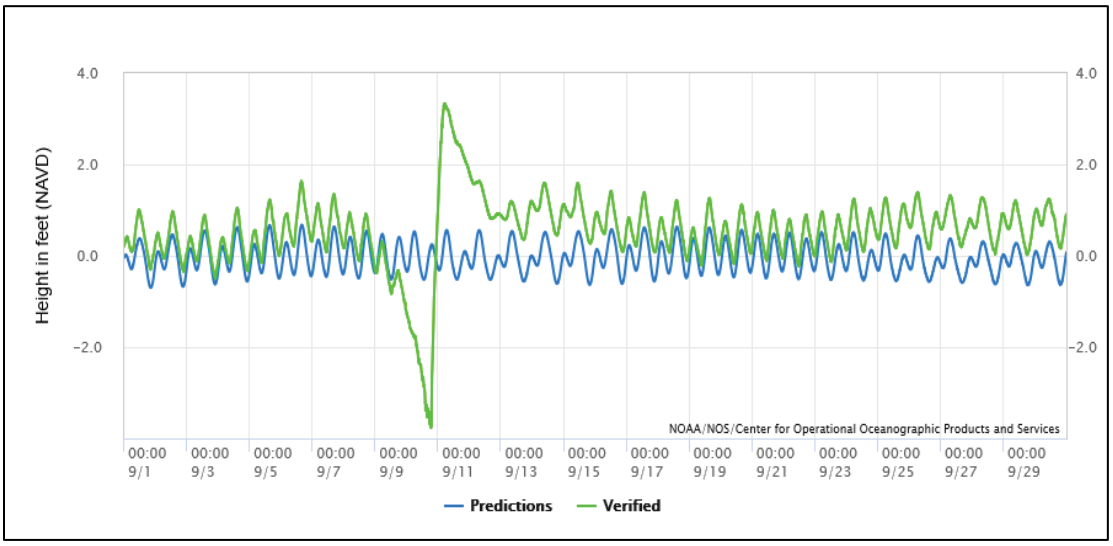

Measured sand volume changes over the course of this project were used to estimate the local sand budget and to provide further insight on the net movement of sediment. Conceptual sediment budgets allow estimates of sediment volume entering and exiting regions by analyzing volume changes over time. Sediment budgets have been regularly used to identify sources and sinks within the littoral zone through a basic mass conservation equation:

$$\sum Qsource - \sum Qsink - \nabla V + P - R = residual \quad (1)$$

The net volume change within each cell (∇V) is used in conjunction with any sediment sources (Q_{source}), sinks (Q_{sink}), sediment placed (P) and sediment removed (R) to determine total change within the given area (Rosati and Kraus 1999). This analysis requires volume measurements through relatively long intervals of time to ensure a stable sand budget that is not biased by short-term variations. However, the sediment budget calculation for this project was performed using volume data over an approximately 17-month period, which is a relatively short period of time. Uncertainties due to seasonal or storm produced volume changes can be averaged out over longer term sand budgets. Zarillo et al. (2015) present examples of short-term and long-term sand budgets that illustrate variability is typical when comparing sand budgets at different time scales for the same coastal region. Shorter-term sand budgets are often difficult to balance without assuming large volumes of onshore or offshore sand movement, which can be more balanced over longer time scales.

Figure 28 shows the annualized sand budget calculation based on the 17-month period from August 2016 to January 2018. The calculation was performed in the Sediment Budget Analysis System based on the sand budget concepts of Rosati and Kraus 1999. Whereas this calculation is not representative of sand budgets in this area over the longer terms of 5 yr and beyond, it is representative of the sediment exchanges among the control and berm areas for the duration of this project. The magnitude of the sediment flux values through the sand budget cells (Q) are, in part, dependent on the initial values of sediment flux (Q_{in}) into the area. There are no recent measurements or datasets that quantify incoming sources or sinks (Q+/-) of sediment into or out of the sediment budget. Thus, the Q transport values are largely calculated in a relative sense based on the measured volume changes. However, the relative sand budget can provide useful information.

The first August 2016 to January 2018 sediment budget assumes that the net transport is to the south and that the initial Q_{in} value was near zero (Figure 28) and the post-storm emergency fill placement of approximately 2,100 cubic yards is included in the budget calculation. The concept of a net southward transport of sediment along the shoreface is supported by the arrival of a large volume of sand in the north control area between May 2017 and September 2017 followed by

loss of most of this volume by January 2018 and a large sand volume gain in the south control area (Figure 26). The patten of this sand volume exchanges is well represented in the topographic plots (Figure 25). The large sand volume fluctuation is not directly represented in the sand budget except as a component that influences the net volume change over the 17-month period.

Figure 28. Results of a sediment budget calculation based on net sediment volume changes measured in the control areas and berm areas between August 2016 and Janauary 2018. Measured volume changes are in cubic yards (dV) and calculated transport values in cubic yards per year (Q) .

A second sand budget calculation shown in Figure 29 presents an alternative that is consistent, with the concept of a reversal in net littoral drift direction at the north end of Estro Island (USACE 1969; Wang et al. 2013). In this alternative a net transport rate of 10,000 yd^3/yr is assumed to directed north out of the north control area. This results in a lower export of sand from the south control area budget cell.

An issue within both of the sand budget alternatives is the large net annualized sand flux between the berm and south control areas that arises when trying to balance the budget. Previous work suggests that

the littoral drift rate along Estero Island is low and on the order of 50,000 yd^3/yr or less rather than the 100,000+ rates intra-area rates shown in Figures 28 and 29. The larger rates in these relatively short-term budgets may be due to the large sand volume moved by the Hurricane Irma that were subsequently removed from the study area according to the topographic and volume calculations. The pathways for some of this volume is movement to south and deposition in the south area, which may be acting as a sand trap due to the lower topographic elevation.

Figure 29. Results of a sediment budget calculation based on net sediment volume changes measured in the control areas and berm areas between August 2016 and Janauary 2018. Measured volume changes are in cubic yards (dV) and calculated transport values in cubic yards per year (Q) .

A way to mitigate the large littoral drift rate between the berm and south control areas is to specify sand loss beyond the base of the shoreface. This would provide an offshore pathway for dispersal from the shoreface of storm-deposited sediment. This alternative renders the south area as a complete sand trap providing no transport to the south as shown in Figure 30. In this case the intra-area net longshore transport rate between the berm are and the south control area is reduced from more than 100,000 yd^3/yr to 71,000 yd^3/yr (Figure 30).

Figure 30. Results of a sediment budget calculation based on net sediment volume changes measured in the control areas and berm areas between August 2016 and Janauary 2018. Measured volume changes are in cubic yards (dV) and calculated transport values in cubic yards per year (Q) .

4.8 Summary of morphological evolution and sand budget

Profile analyses and topographic surveys, as well as sand volume change analyses, show that the beach and upper shoreface within the berm area was mostly accretional as the berm sediments migrated onshore and welded onto the shoreface and remained stable though Hurricane Irma (Figure 17 and Figure 25). This provides evidence that sediments in the nearshore berm readily adjusted to variations in wave energy including a rebound to the pre-storm grain size distribution as seen in Figure 8. The onshore migration of the Berm is readily observable in Figure 25, showing the net topographic changes between August2016 and January 2018.

Overall, the north control area and the lower shoreface in the berm area lost sediment volume through the survey period whereas the South control area gained sediment volume through all time periods except in the post-storm period from September 2017 to January 2018. The large sediment volume changes around the storm may be due to sediment

inputs from the effects of storm-surge-produced scouring of nearby bay and estuarine channels. The ability of the South control area to persistently acquire sand volume may be linked to its topographically lower elevation controlled by the underlying carbonate surface.

Sand budget calculations reflect the measured sediment volume changes and the time period over which the calculations are made. The three alternative sand budget calculations differ in the details depending on how each budget is balanced using assumed sand volume transport rates at the boundaries. However, all sand budgets demonstrate that over the 17 months of the study, budgets are consistent with sand volume loss from the north control and berm areas and corresponding sand volume gains the south control, which acted as a sediment trap retaining much of the sand arriving from the north.

4.9 Shoreline changes

One possible benefit to placement of a nearshore berm is added protection of the beach at the shoreline. Under the right conditions, a nearshore berm can dissipate wave energy and therefore could reduce shoreline recession. This section focuses on the historical movement of the shoreline including changes pre- and post-construction of the 2009 nearshore berm (Figure 31. Location of all shorelines, baseline, and transects used in DSAS. Shorelines representing different dates of lidar imagery are shown in legend (Enfinger 2018). A shoreline change assessment for the years of 1998 to 2015 show an overall shoreline accretion (Figure 32). The largest movement is seen in the berm area and north control area (+3.29 to +13.12 ft/yr) whereas the south control area shows smaller amounts of seaward movement (+0.1 to 3.28 ft/yr). The period of 1998 to 2015 was influenced by two renourishments (2001 and 2011) and the placement of the 2009 nearshore berm.

Figure 31. Location of all shorelines, baseline, and transects used in DSAS. Shorelines representing different dates of lidar imagery are shown in legend (Enfinger 2018).

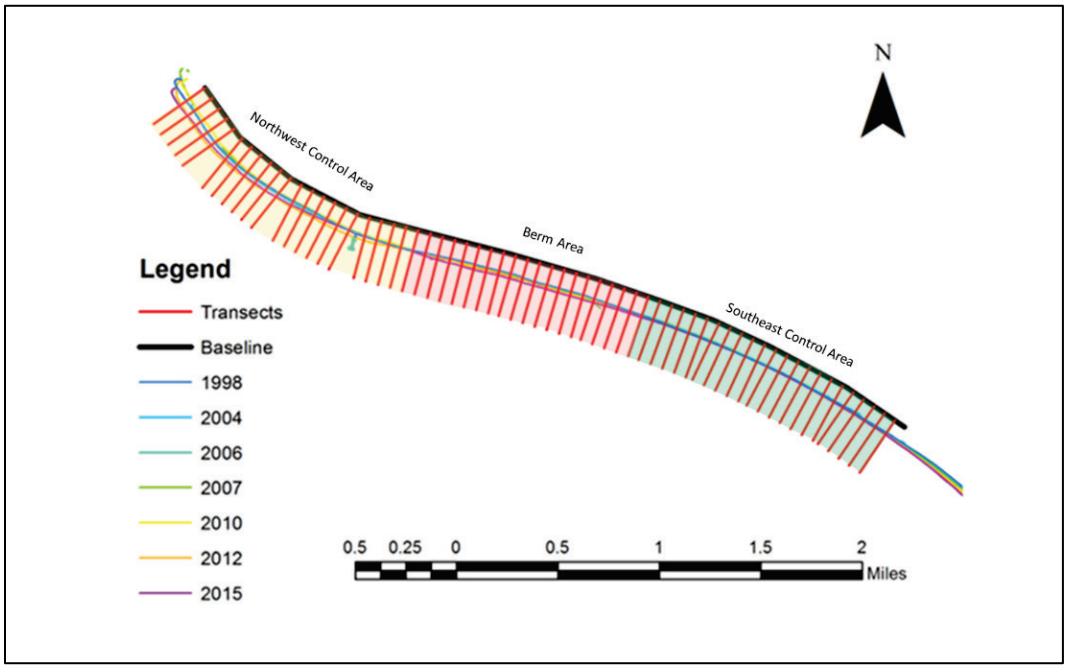

Figure 32. Map displaying EPR for the years 1998 to 2015 (Enfinger 2018).

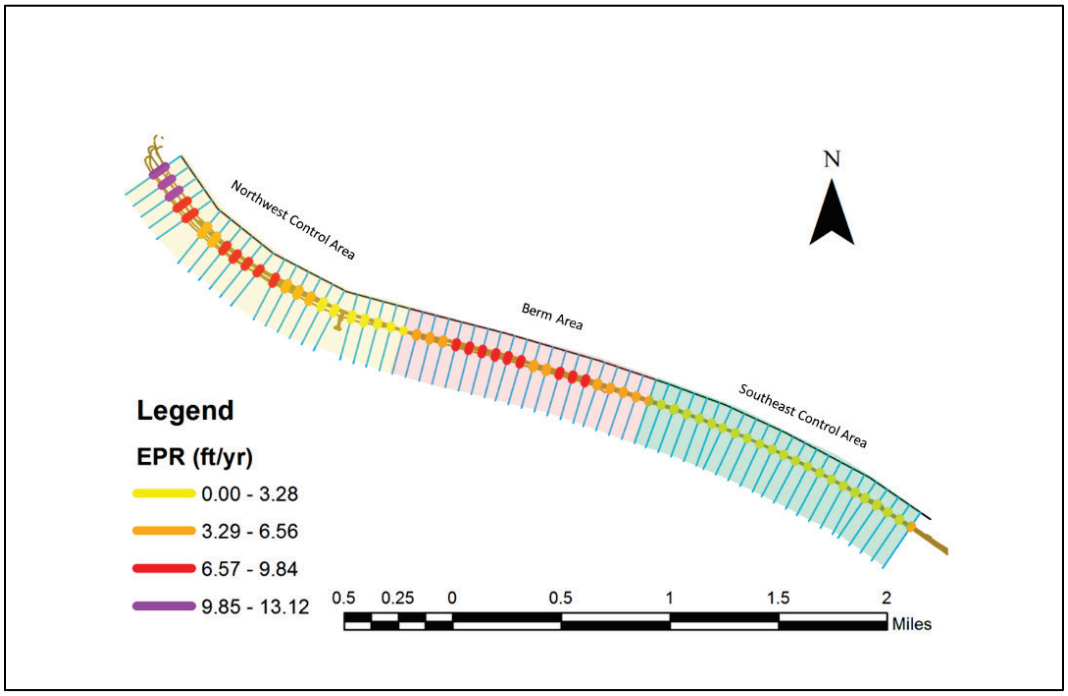

Prior to berm construction in 2009 (1998 to 2007), the study area showed both shoreline recession and accretion (Figure 33). Erosional hotspots occurred close to the pier in the northern portion of the berm, the central portion of the north control area, and the northern portion of the south control area at a rate of -0.1 to -3.28 ft/yr. The greatest shoreline recession occurred within the north control area totaling -26 ft within the time period. The greatest accretion occurred within the central portion of the berm at a rate of +3.29 to +6.56 ft/yr.

Figure 33. Map displaying EPR for the pre-nearshore berm, years 1998 to 2007 (Enfinger 2018).

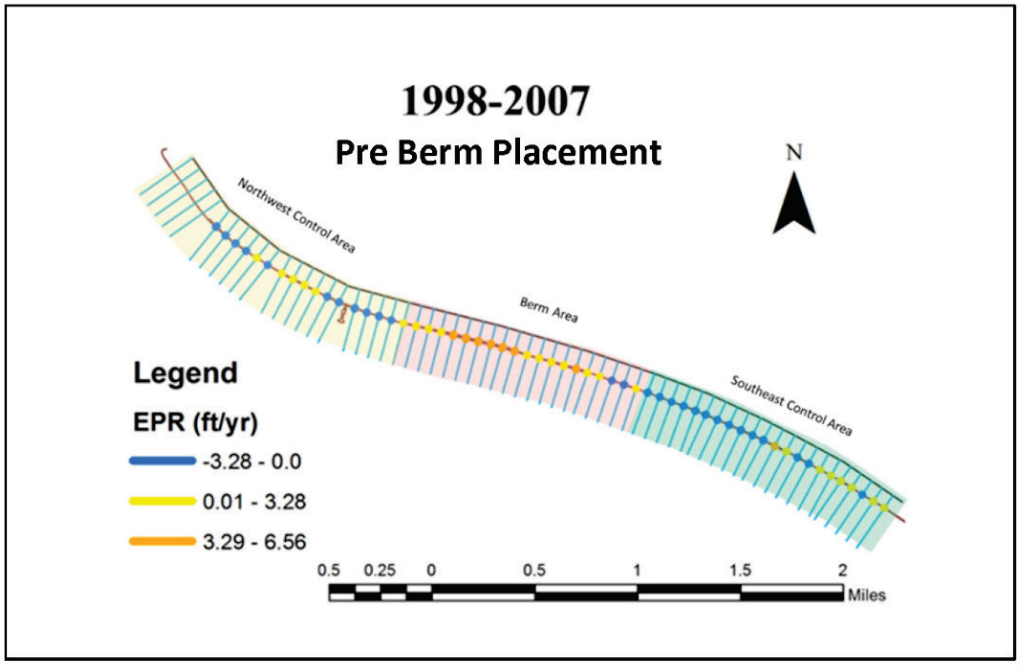

After construction of the 2009 berm (2010 to 2015), the entire extent of the shoreline showed consistent accretion (Figure 34). The least amount of shoreline accretion occurred within the south control area at a rate of +0.1 ft/yr to +6.56 ft/yr whereas the shoreline within the berm area showed accretion between +6.56 ft/yr and 19.69 ft/yr. The largest amount of accretion occurred in the north control area ranging from +19.7 ft/yr to 72.18 ft/yr. This was likely due to the beach nourishment within that area in 2011.

Figure 34. Map displaying EPR for the post nearshore berm years 2010 to 2015 (Enfinger 2018).

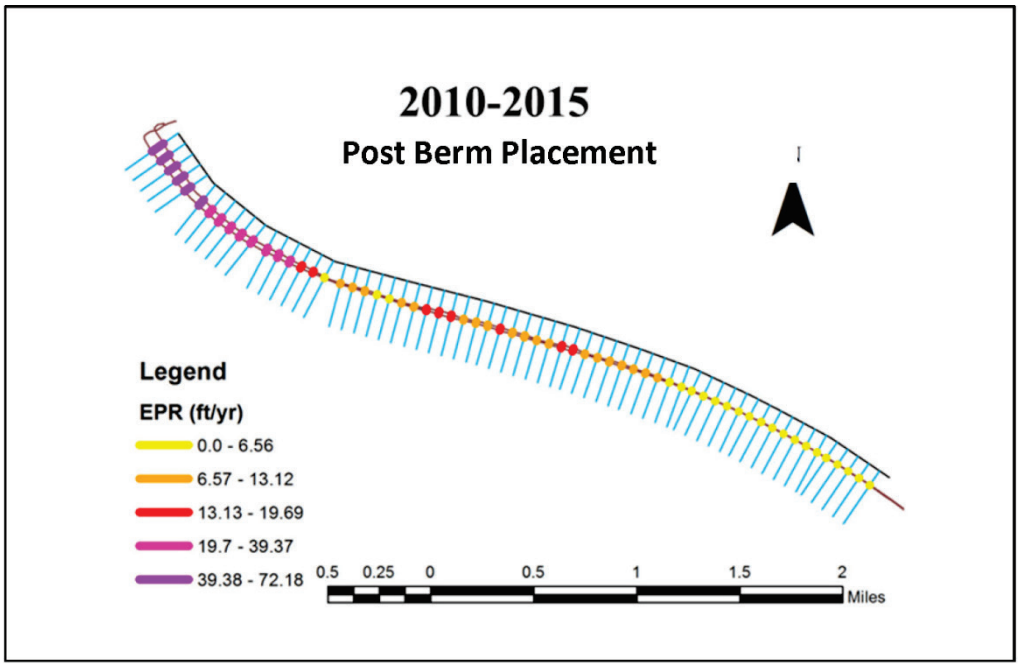

The shoreline mapped from the 2015 lidar survey and the shoreline extracted from the final topographic survey of this study completed in January 2018 are compared in Figure 35. It can be seen that the shoreline mapped as the NAVD 88 zero contour is mostly seaward of the 2015 shoreline within the berm area. To further illustrate the difference in the shoreline positions, the net change between the 2015 and 2018 shoreline is shown in Figure 36. The shoreline change is plotted according to alongshore distance from the northwest to southeast end of Fort Myers Beach. Shoreline retreat is noted in the first alongshore mile and then reverses to dominantly shoreline advance for the length of the berm location. The pattern then reverses to shoreline retreat along the first 2,000 ft to the southeast of the berm. Along the 4,000 ft southeast section of the study area, the January 2018 shoreline reached a maximum of approximately 20 ft Gulfward beyond the 2015 NAVD88 shoreline.

An update of the shoreline position since the berm placement in August of 2016 shows that the Fort Myers Beach shoreline may have been influenced by the berm (Figure 35). The shoreline along the Berm area advanced Gulfward (Figure 36) whereas the shoreline position to the north and immediately to the south retreated. It is noted that the sand

volume contained in the berm has undergone an overall landward shift since 2016 (see Figure 17 and Figure 25) and likely resulted in additional shoreline stability during this period.

Figure 35. Comparison of the 2015 NAVD88 00 ft contour contour based on lidar data with the January 2018 0 ft contour based on RTK survey data.

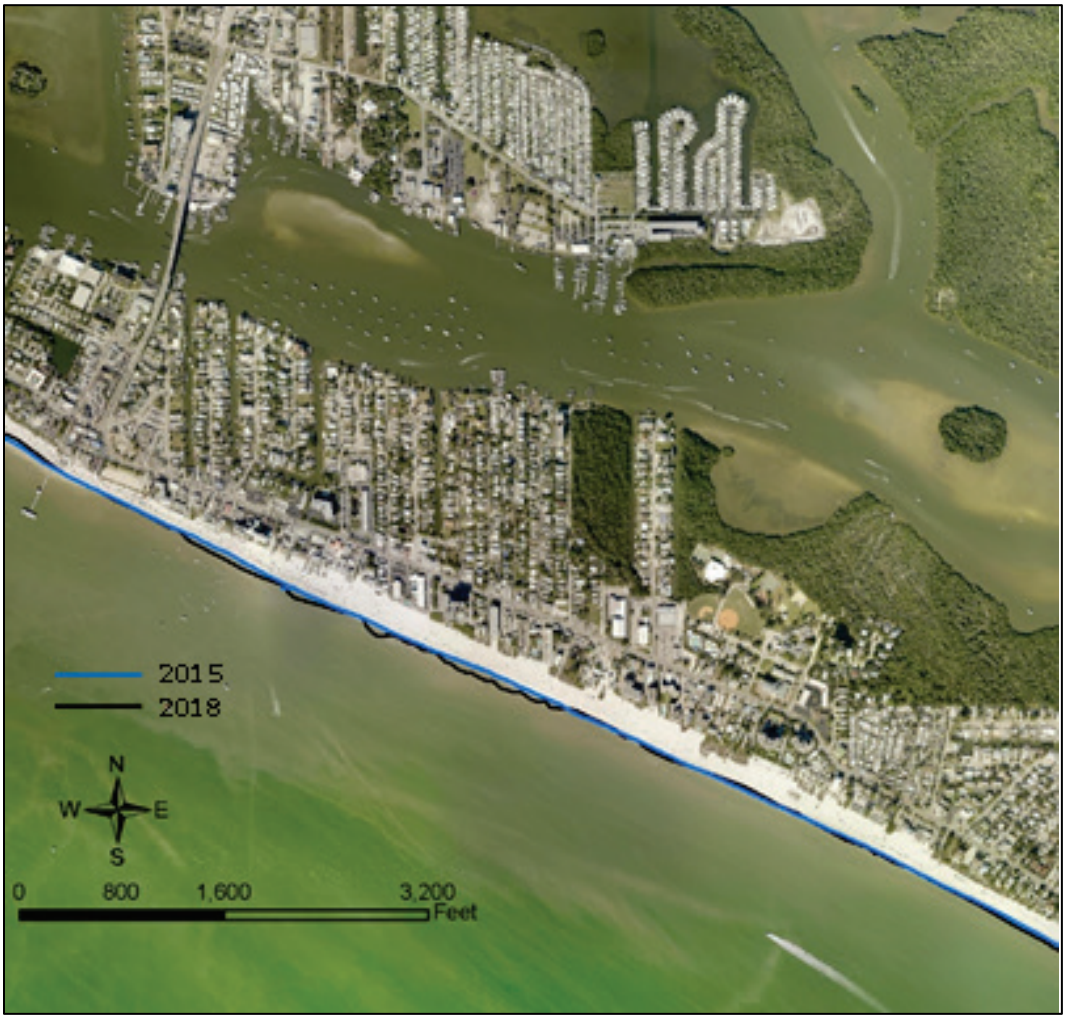

Figure 36. Change in shoreline position calculated from the 2015 lidar survey and the final Janaury 2018 survey conducted for this study. The location of the berm area is shown. Alongshore distance values are from north to south.

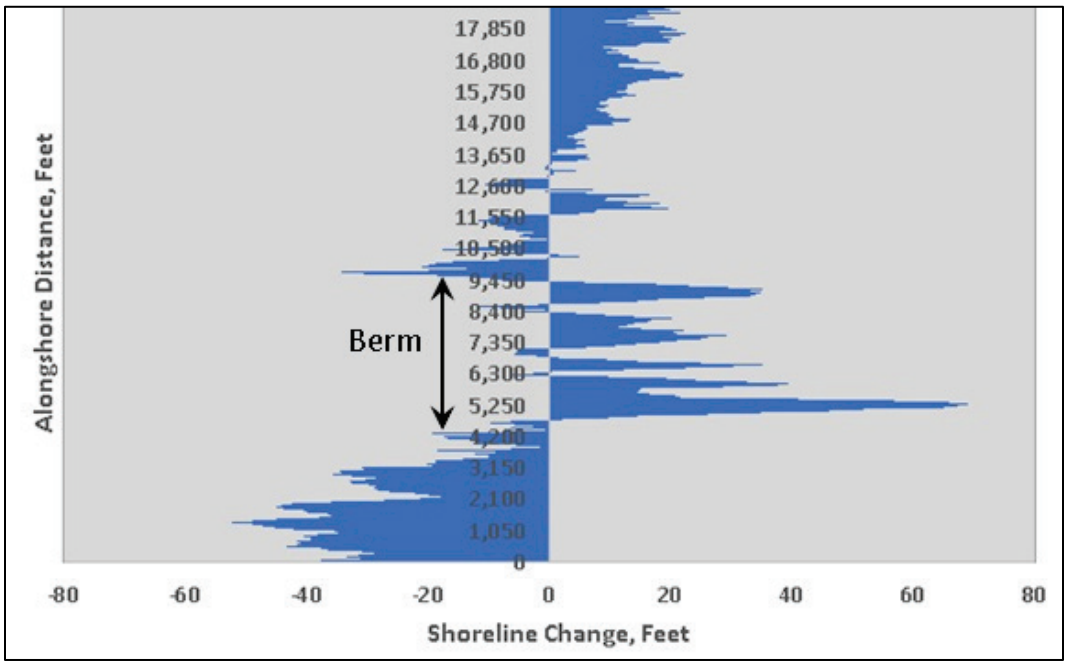

4.10 Summary of shoreline changes

By comparing pre-berm to post-berm shoreline positions, it can be seen that some segments of beach in the study area experienced recession whereas in the post-2011 beach nourishment period through 2015, the shoreline along all sections of beach was stable or accreting. The average shoreline accretion rate in the berm area in the 2010 to 2015 period was higher than in the pre-berm period. Changes since berm construction in in 2016 indicate shoreline stability in the berm area compared to shoreline retreat immediately to the north and south of the berm area.

5 Discussion

Sedimentological and topographic data collected in this study were applied to several related analyses designed to examine the performance of the nearshore berm placed along the middle section of Fort Myers Beach, Florida. This study complements the analysis of a similar berm placed at Fort Myers Beach in 2009 (Brutsché 2011, 2014; Wang et al. 2013) and includes the analysis of the performance of the most recent berm constructed in the summer of 2016. This assessment includes analysis of sediment distribution, morphological evolution, sediment transport, and effects of the nearshore berm on the adjacent shoreline. Additionally, historical shoreline trends were analyzed. An important component of this study is a comparison of the section of Fort Myers Beach where the berm was placed with control sections of the beach and shoreface to the north and south. In this study the south control area was extended farther south along Fort Myers Beach in comparison to previous studies. This was an advantage in capturing the influence of the underlying geologic formations on morphology of the study area and providing an opportunity to examine longshore sediment transport in the sand budget analyses.

The sedimentological analyses combine a description of sediment grain-size distribution across the beach and shoreface with supporting statistical analyses to test sedimentologic differences in space and time. This combined analysis is benefited by the imprint of Hurricane Irma in early September 2017 immediately after which sediment samples and topographic data were collected.

Based on the three sediment sample data sets in sub-sections of the study area (north, berm, and south areas), the storm produced an increase in percentage of very fine sand on the mid to lower shoreface and a corresponding decline in the percentage of fine sand. This signature was present in all three study sub-sections. The post-storm sediment analysis showed that the relative abundances of fine and very fine sand largely reversed back to the May 2017 pre-storm pattern of higher percentages in the fine sand classes and lower percentages in the very fine sand size classes.

Since beach and shoreface sediments in the Fort Myers area are well sorted (poorly graded in engineering terms), shifts in grain size

distribution even under storm conditions can seem moderate but are made more apparent by statistical properties of the sediment size distribution. In this case, statistical testing indicated that there was a significant difference in modal grain size over the entire study among the pre- and post-storm sampling periods. More detailed statistical testing on the sediments indicated where and when statistical differences occurred among the three study area sub-sections and support the visual difference in grain size distributions that can be seen in Figures 7 to 9. Statistical tests confirmed interpretations of the impacts on study area sediments by Hurricane Irma. For instance, statistical testing of modal grain size differences by area and elevation in the May 2017 sediment data confirm what is inferred about the cross-shore distribution of sediment grain sizes. Further, testing of the May sediment data indicates a statistical difference in modal grain size among the sub-areas. The same statistical tests by elevation and area conducted on the September 2017 sediment data again confirmed the observed cross-shore distribution of sediment grain size but indicated modal grain size similarity among the three study sub-sections (north, berm, and south). This could be interpreted as mixing or imprinting of Hurricane Irma on the sediment over all three areas.

Testing of the January 2018 sediment data showed that statistically the modal gain size abundances in all study area sub-sections returned to the pre-storm condition of being statistically different in terms of and area and elevation. This indicates that the study areas largely re-equilibrated to non-storm conditions and tested in a similar way as the May 2017 sediment data set.

The abundance of fine-grained sediments (<0.06 mm) is of concern in any project to restore the coast by fill placement and is reason for placing the material dredged from Matanzas Pass offshore of Fort Myers Beach. Fine-grained sediment percentages were tracked through the study and examined on a spatial and temporal basis. One of the important findings of this study is that fine, silty sediments were very abundant in the south control area through the entire sampling period. Percent fines were typically in the range of 30% to 60% by weight on the lower shoreface through all three sampling periods. This persistent abundance is potentially linked to a fine carbonate fraction derived from scouring of the underlying carbonate-rich formations just below the

modern topographic survey and intermittently exposed in the south control area.

In the berm area, the May 2017 samples contained a noticeable fine grain sediment distribution extending from the base of the shoreface at -10 ft to a depth of -2 ft, along with a trace of fines on the beach in the range of 3% . This is likely the result of silts winnowed out of the dredged material used to construct the berm and known to contain approximately 10% to 20% fine material. Likewise, in the May 2017 data set, the north control area on the average included a fine-grained sediment fraction in a range of approximately 5% to 8% extending from the base of the shoreface onto the beach.

The signature of Hurricane Irma on the fine-grained sediment was an overall reduction in abundance of fine-grained sediment in all three sub-sections of the study area. The remaining post-storm fine sediment percentages were most noticeable on the lower shoreface. However, the sediment percentage remained high in the south control area at the base of the shoreface at depths of -8 to -10 ft. The percentage of fines increased to approximately 25% in the north control are at the base of the shoreface. The pattern of fine sediment distribution remained about the same in the January 2018 sample data, except for the removal of most of fine-grained sediment at -10 ft in the north control area. Thus, the storm impact and higher energy conditions leading into the winter months resulted in reworking of the fine sediment fraction off the upper shoreface and deposition of fines on the lower shoreface.

Statistical testing of fine-grained sediment abundance confirmed the interpretation of the observed abundance through the study area. Fine-grained sediment abundance found among the three sub-areas of the study in the May 2017 data set, were statistically different than the fine sediment content of the September 2017 and January 2018 sample data. Further, statistical tests supported the observation that fine-grained sediment was spread more widely across the shoreface in the May 2017 samples before Hurricane Irma. However, after the storm, fine-grained sediment concentrations across the shoreface were statistically different in accordance with the observed highest concentration located at lower elevations.

Analysis of the topographic survey data provides a quantitative evaluation of how changing sediment distributions across the beach and shoreface is linked to sources and sinks of sediment. The topographic data from the south control area also provided a previously unknown contrast with the topography of the north control area and berm area. The major features of the topographic analysis include net erosion in the north control and berm areas in combination with a relatively large sediment volume gain of approximately 193,000 yd^3 in the south area. Net sand volume gains in the south area approximately balanced the total of approximately 218,000 yd^3 of volume loss in the north and berm areas over the life of the study. This balance is reflected in the evolution of topographic profiles in each of the study area sub-sections. The mid- to lower shoreface topographic profiles in the north control area and berm area lost elevation whereas the elevation of the mid- to lower shoreface in south control area increased by more than a foot. An exception to this pattern was a temporary increase in the lower shoreface elevation in the north area seen in the post-storm September 2017 data. The source of the approximately 250,000 yd^3 of sediment arriving in the north control area is unknown but could be derived from flushing of sediment from Estero Bay and natural and navigational channels connecting the interior bays and estuaries.

However, by January 2018, the elevation of the mid- to lower shoreface of the north area dropped by a foot or more. Sediment volume shifts among the sub-sections are particularly apparent in net topographic changes presented in Figure 25, which shows lowering of elevation over time in the north and berm areas and increased elevation in the south area. Also apparent in Figure 25 is the onshore migration of berm on the upper shoreface. The shoreline change pattern between 2015, and the final survey of January 2018 is consistent with volume and elevation changes as shown in Figure 25. The 2018 shoreline migrated Gulfward within the berm area and mostly retreated landward in the adjacent areas.

The three alternative sand budgets for the study area differ in their assumed boundary conditions that set sand flux into and out of the budget cells. However, the sand budget alternatives are largely defined by measured sand volume changes among the budget cells. In each of the sand-budget calculation results, the south control area serves as a sediment catchment basin where most of the sand eroded from the

north and berm areas is deposited. Specific sediment boundary conditions determine whether the south area exports a small amount of sediment volume to the south or retains all sand volume arriving from the north. Sand budget calculations based on sand volume changes over the 17-month study period may not reflect longer-term sediment dynamics over 5 to 10 yr periods. However, the ability to accumulate and rapidly disperse sand volume as demonstrated in the two post-storm topographic surveys may indicate that the Fort Myers Beach area is in approximate dynamic equilibrium in the longer term and on the average subject to relatively low rates of littoral drift.

6 Conclusions and Recommendations

This study considers sediment distribution, morphological evolution, sediment transport, and shoreline trends of the Fort Myers Beach area with respect the construction of the nearshore berm in August of 2016. Due to timing of field study, this report also includes an analysis of the influence of a major hurricane that impacted the area in September of 2017. The nearshore berm was constructed with 130,000 yd^3 of sediment dredged from Matanzas Pass, which contained more fine-grained material than is allowed to be directly placed on the subaerial beach. Thus, the dredged sediment was placed in the nearshore.

Conclusions about the performance of the Fort Myers Beach berm over the course of this study can be made in the context of the sedimentologic and morphologic evolution of the berm area and the adjacent north and south control areas. Further, the imprint of Hurricane Irma in September 2017 provided a rare opportunity to observe the sedimentologic and morphological response across the study at the event time scale.

Sedimentologically, the berm area is similar to both control areas in being dominated by fine and very fine sand over most of the shoreface and beach. Fine sand dominates the upper shoreface and beach whereas very fine size classes dominate the lower shoreface in all three study sub-sections. At the beginning of the study, the distinctive sedimentologic signature in the berm area was a fine-grained sediment fraction (<0.06 mm) distributed across the shoreface all the way to the shoreline in percentages of 5% to 10%. In contrast, most of the higher percentages of fine-grained sediment were confined to the lower shoreface in the other sections. The high percentages of fine-grained sediment in the south control area that persisted through the study are potentially related to the much higher percentage of carbonate sediments in this area indicating the proximity of the underlying older geological formations to the surface that may be contributing fine-grain material to surficial sediments.

Analysis of sediment size fractions over time leads to the conclusion that there was a sedimentological variation cause by the Hurricane Irma in which the abundance of very fine sand temporarily increases across the shoreface in all three study sub-areas, along with a corresponding

decline in the abundance of fine sand on the upper shoreface. The source of the increase in very fine sand is unknown, but considering the large increase in sediment volume in all three areas documented in the first post-storm survey, fining of surficial sediment can be potentially linked to fine sediment resuspended in Estero Bay the storm, exported from Matanzas Pass, and settling over the Fort Myers Beach Shoreface. In the second post-storm sediment data set, the distribution of fine sand and very fine sand reverted to the pre-storm pattern potentially as a result of reworking by increasing wave energy as the winter months approach.

Relatively high percentages of silt in the berm area just after construction of the berm were apparently removed by the storm even as the presence of very fine sand increased. Since the cross-shore distribution of high silt percentages was not present in the January 2018 sediment data, it is concluded that the storm reworked the silt fraction from the original berm sediments during the ongoing process of adjustment to equilibrium on the shoreface.

From the topographic evidence, it can be concluded that the berm went through a morphologic evolution of migrating onshore across the upper shoreface and welding onto the foreshore of the beach. Much of this evolution was complete by the time of the May 2017 survey. Hurricane Irma did not have a significant impact on the morphology of the upper shoreface in the berm areas as seen in a relatively wide beach berm in the September 2017 topographic data. However, at the time of the January 2018 topographic survey, the wide beach berm was cut back, and a nearshore bar was developing. From this is it concluded that by the close of the data collection period 17 months after construction of the berm, sediments and morphology had largely equilibrated with the physical setting of Fort Myers Beach.

From the analysis of the change in shoreline position between the lidar survey of 2015 and final topographic survey of January 2016, it can be concluded that the berm provided a source of sand nourishment for the upper shoreface and beach. This is apparent in the profile analysis shown in Figure 17 and the topographic surface analysis presented in Figure 25.

The sand volume analysis and sand budget alternatives indicate that sediments eroded in the north sections of the study area are, in part, captured in the topographically lower south section of the study area. The lower elevation of the south control area is observable in the time-averaged topographic profiles shown in Figure 19.

The overall conclusion of this study is the Fort Myers Beach berm has performed well in terms of mitigating erosion of the upper shoreface and preventing shoreline retreat. Further, the sedimentological and topographic analysis of this study leads to a recommendation of how to reproduce the success of the 2016 Fort Myers berm project and extend this success to other areas. The response of the project area to Hurricane Irma and the post-storm sedimentologic rebound is a reminder that sediment grain-size distribution across the shoreface and beach is a product of both available sediment sources and the physical setting. To maximize performance of a constructed berm it is recommenced that in a nearshore berm project area, a detailed sediment survey be conducted across the project shoreface along with a survey of the sedimentologic indices of the source material. A combined analysis of the cross-shore distribution of sediment grain size with the distribution of sediment size in the construction material can be used to perform a check on the compatibility of the construction sediments with the placement location in the project area. This is analogous, in concept, to beach sand compatibility analysis methods described by Bodge (2006), Dean (1974), and James (1975) except applied to optimize the cross-shore location of borrow sediments.

There is a large body of literature on grain-size partitioning across a wave-dominated shoreface. Examples by Liu and Zarillo (1993) and Zarillo et al. (1985) demonstrate how this knowledge can be applied to evaluate the grain-size distribution of a potential sand source for stability and eventual redistribution on the shoreface under prevailing physical conditions.

A final recommendation is to continue topographic and sediment surveys in the Fort Myers Beach study area to complete the analysis of the berm performance. Ideally, surveys on an annual basis should continue to at least 10 yr beyond original construction of the berm. This would allow a complete analysis of a longer-term sand budget and the equilibrium sediment distribution in the area after placement of the

berm sediments and impact of Hurricane Irma. In the case of another major storm, a post-storm survey is recommended. In the case of any future linkage between berm construction and dredging of Matanzas Pass, a pre-construction survey of sediments to be excavated is recommended to optimize the location of the berm on the Fort Myers Beach shoreface.

References

Bodge, K. R. 2006. "Alternative Computation of Dean's Overfill Ratio." *Journal of Waterway, Port, Coastal, and Ocean Engineering* 132: 133–138.

Brutsché, K. E. 2011. *First Year Sedimentological Characteristics and Morphological Evolution of an Artificial Berm at Fort Myers Beach, Florida*. Master of Science thesis. University of South Florida.

Brutsché, K. E. 2014. *Evolution and Equilibration of Artificial Morphologic Perturbations in the Form of Nearshore Berm Nourishments Along the Florida Gulf Coast*. University of South Florida.

Cangialosi, J., A. Latto, and R. Berg. 2018. "Hurricane Irma." *NOAA National Hurricane Center Tropical Cyclone Report*, June, 111. http://www.nhc.noaa.gov/data/tcr/AL112017_Irma.pdf

Coast & Harbor Engineering. 2015. *Coastal Management Plan Development Fort Myers Beach, Florida*. February 5. Coast & Harbor Engineering.

Coastal Engineering Consultants, Inc. 2015. *Estero Island Restoration 2015 Annual Monitoring Report*. Lee County Board of County Commissioners and Florida Department of Environmental Protection.

Dean, R. G. 1974. "Compatibility of Borrow Material Texture for Beach Fill." *Proc., 14th Int. Conf. on Coastal Engineering*, ASCE, Reston, VA, 1319–1333.

Enfinger, K. 2018. "Morphologic Evolution of a Nearshore Berm: One Year Monitoring at Ft. Myers Beach, Florida." Master of Science thesis. Florida Institute of Technology.

ESRI. 2016. "How Natural Neighbor Works." *ArcGIS for Desktop*. http://desktop.arcgis.com/en/arcmap/10.3/tools/spatial-analyst-toolbox/how-natural-neighbor-works.htm.

Heiri, O., A. Lotter, and G. Lemcke. 1999. "Loss on Ignition as a Method for Estimating Organic and Carbonate Content in Sediments: Reproducibility and Comparability of Results." *Journal of Paleolimnology* 25(November): 101–10.

Himmelstoss, E. A., R. E. Henderson, M. G. Kratzmann, and A. S. Farris. 2018. *Digital Shoreline Analysis System (DSAS), Version 5.0 User Guide*. US Geological Survey Open-File Report 2018–1179. https://doi.org/10.3133/ofr20181179.

Hine, Albert C. 2013. *Geologic History of Florida: Major Events that Formed the Sunshine State*. Gainesville, FL: University of Florida Press.

James, J. R. 1975. *Techniques in Evaluating Suitability of Borrow Material for Beach Nourishment*, Technical Memorandum No. 60. Vicksburg, MS: Coastal Engineering Research Center, US Army Engineer Waterways Experiment Station.

Liu, J. T., and G. A. Zarillo. 1993. "Simulation of Grain-Size Abundances on a Barred Upper Shoreface." *Marine Geology* (109): 237–251.

Missimer, T. 1992. *Stratigraphic Relationships of Sediment Facies within the Tamiami Formation of Southwest Florida: Proposed Intraformational Correlations*. https://www.researchgate.net/publication/279750874_Stratigraphic_relationships_of_sediment_facies_within_the_Tamiami_Formation_of_Southwest_Florida_Proposed_intraformational_correlations

Montague, C. L. 2008. "Recovering the Sand Deficit from a Century of Dredging and Jetties along Florida's Atlantic Coast: A Reevaluation of Beach Nourishment as an Essential Tool for Ecological Conservation." *Journal of Coastal Research* 244 (July): 899–916. https://doi.org/10.2112/06-0710.1.

NOAA (National Oceanic and Atmospheric Administration). 2017. *DigitalCoast*. NOAA Office for Coastal Management. https://coast.noaa.gov/digitalcoast/

NOAA. 2018. *National Data Buoy Center*. https://www.ndbc.noaa.gov/.

Otay, E. N. 1994. *Long-Term Evolution of Disposal Berms*. PhD Dissertation. University of Florida.

Ramos, S., and G. Zarillo. 2019. "Variation Analysis of Littoral Sediment Associated with a Nearshore Berm." *Coastal Sediments 2019*, June: 857–869. https://doi.org/10.1142/9789811204487_0075.

Rosati, J., and N. Kraus. 1999. *Formulation of Sediment Budgets at Inlets*. Coastal Engineering Technical Note IV-15. Vicksburg, MS: US Army Corps of Engineers, Waterways Experiment Station.

Scott, T., K. Campbell, F. Rupert, J. Arthur, T. Missimer, J. Lloyd, W. Yon, and J. Duncan. 2002. *Geological Map of the State of Florida - Southern Peninsula*. *Geological Map*. USGS. https://ufdc.ufl.edu/UF00015087/00001.

Sellards, E. H. 1919. *Geologic Sections across the Everglades of Florida*. Florida Geological Survey.

Siegel, S., and J. Castellan. 1988. *Nonparametric Statistics for the Behavioral Sciences,* 2nd ed. New York: McGraw-Hill.

Smith, E. R., M. Mohr, and S. A. Chader. 2017. "Laboratory Experiments on Beach Change due to Nearshore Mound Placement." *Coastal Engineering* 121(March): 119–28. https://doi.org/10.1016/j.coastaleng.2016.12.010.

Sokal, R., and J. Rohlf. 1995. *Biometry: The Principles and Practice of Statistics in Biological Research,* 3rd ed. State University of New York at Stony Brook: W.H. Freemand and Company New York.

State of Florida, Department of State. 2010. *Bureau of Beaches and Coastal Systems-Rules and Procedures for Using Sand-Filled Geotextile Dune Cores* (Permits for Construction and Maintenance). Vol. 62B.

Stewart, S. 2017. *Hurricane Matthew*. NOAA National Hurricane Center.

Thieler, R., E. Himmelstoss, J. Zichichi, and A. Ergul. 2009. *The Digital Shoreline Analysis System (DSAS) Version 4.0 - An ArcGIS Extension for Calculating Shoreline Change*. 2008–1278. Open-File Report. Reston, VA: USGS.

USACE (US Army Corps of Engineers). 1969. *Beach Erosion Control Study on Lee County, FLA*. Lee County, Florida: US Army Corps of Engineers, Jacksonville District.

_____. 2012. *Maintenance Dredging Fort Myers Beach Harbor with Beach and Nearshore Placement*. Lee County, Florida: US Army Corps of Engineers, Jacksonville District.

USGS (US Geological Survey). 2001. *A Summary of Findings of the West-Central Florida Coastal Studies Project*. USGS Open File Report 01-303. Reston, VA: USGS.

Wang, P., K. E. Brutsché, J. W. Lagrone, T. M. Beck, J. D. Rosati, and L. S. Lillycrop. 2013. *Performance Monitoring of a Nearshore Berm at Fort Myers Beach, Florida: Final Report*. ERDC/CHL TR-13-11. Vicksburg, MS: US Army Engineer Research and Development Center.

White, W. 1970. "The Geomorphology of the Florida Peninsula." *Florida Geological Survey Bulletin* 51: 164.

Zarillo, G. A., J. T. Liu, and H-S. Tsien. 1985. "A New Method for Effective Beach-Fill Design. Coastal Zone '85." *The Fourth Symposium on Coastal and Ocean Management, Amer. Soc. Civil. Eng*. (1): 985–1001.

Zarillo, G., I. Watts, L. Erickson, K. Hall, and K. Enfinger. 2015. *An Assessment of Inlet Morphologic Processes, Shoreline Changes, Sediment Budget and Beach Fill Performance*. Technical Report. Sebastian Inlet District, Florida.

Appendix: Profile Figures

Figure 37–Figure 42 present cross-shore beach and shoreface profile plots representing the north, berm, and south control areas.

Figure 37. Cross-sectional profile of transect FMB7 for all dates collected. Transect is located in the southeast control area.

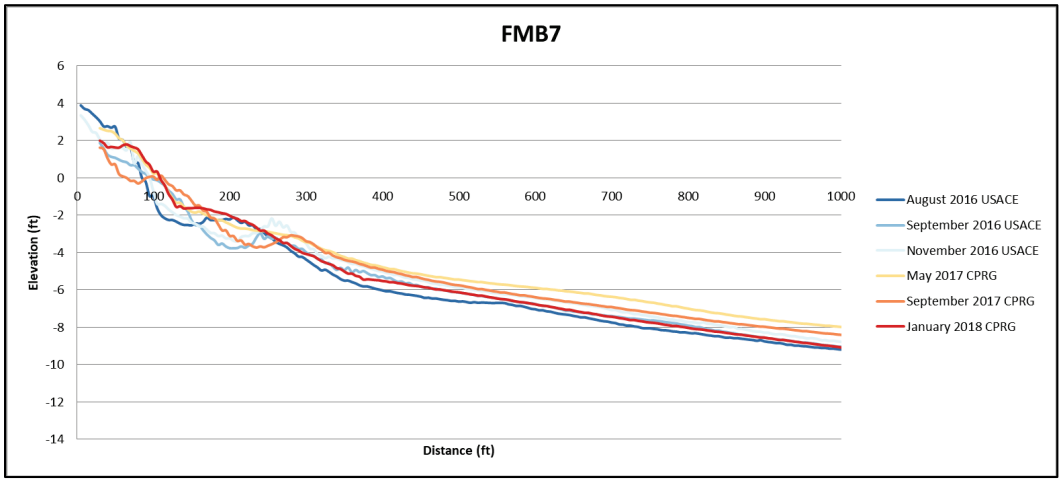

Figure 38. Cross-sectional profile of transect FMB 9 for all dates collected. Transect is located in the southeast control area.

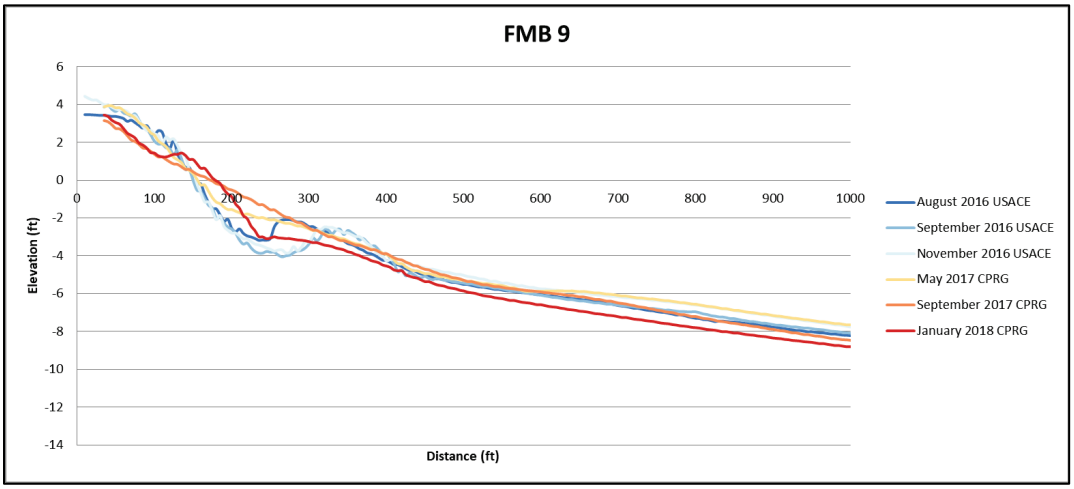

Figure 39. Cross-sectional profile of transect FMB 23 for all dates collected. Transect is located in the nearshore berm area.

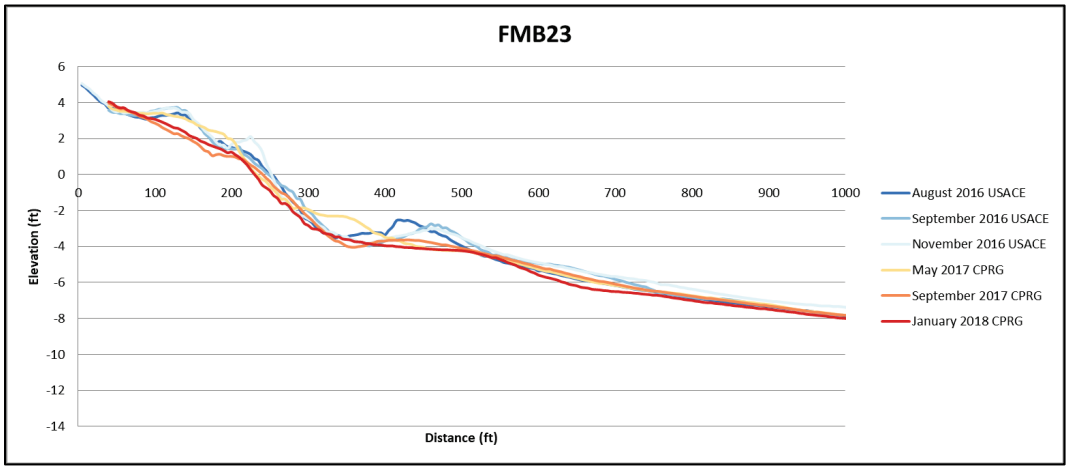

Figure 40. Cross-sectional profile of transect FMB 35 for all dates collected. Transect is located in the nearshore berm area.

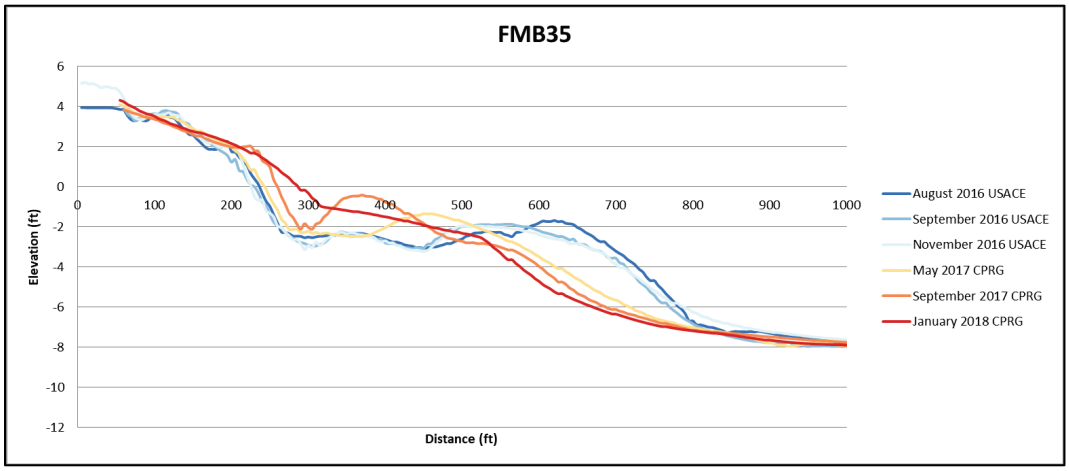

Figure 41. Cross-sectional profile of transect FMB 51 for all dates collected. Transect is located in the north control area.

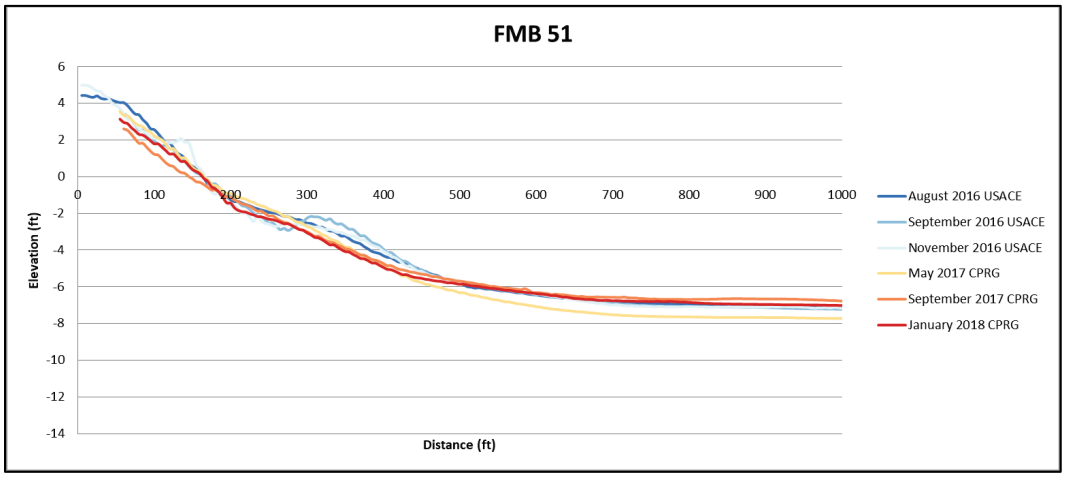

Figure 42. Cross-sectional profile for transect FMB 54 for all dates collected. Transect is located in the north control area.

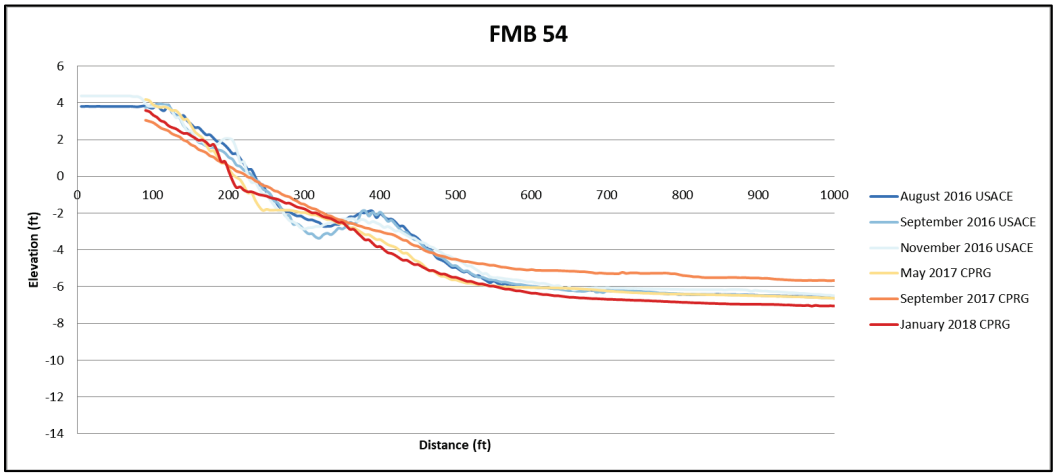

Unit Conversion Factors

Multiply	By	To Obtain
cubic yards	0.7645549	cubic meters
feet	0.3048	meters
yards	0.9144	meters

Acronyms and Abbreviations

ANOVA	Analysis of Variance
CPRG	Coastal Processes Research Group
DSAS	Digital Shoreline Analysis System
EPR	End point rate
FDEP	Florida Department of Environmental Protection
GNSS	Global navigation satellite system
KFMY	Fort Myers Page Field Airport
NOAA	National Oceanic and Atmospheric Administration
RTK	Real-time kinematic
USACE	US Army Corps of Engineers

REPORT DOCUMENTATION PAGE

Form Approved
OMB No. 0704-0188

1. REPORT DATE	2. REPORT TYPE	3. DATES COVERED *(From - To)*
March 2022	Final Report	

4. TITLE AND SUBTITLE
Evaluating Cross-Shore Sediment Grain Size Distribution, Sediment Transport, and Morphological Evolution of a Nearshore Berm at Fort Myers Beach, Florida

5a. CONTRACT NUMBER

5b. GRANT NUMBER

5c. PROGRAM ELEMENT NUMBER

6. AUTHOR(S)

Gary A. Zarillo, Sara A. Ramos, Kristopher Effinger, Kristen Becker, Irene Watts, Katherine E. Brutsché, Brian C. McFall, and Douglas R. Krafft

5d. PROJECT NUMBER

5e. TASK NUMBER

5f. WORK UNIT NUMBER

7. PERFORMING ORGANIZATION NAME(S) AND ADDRESS(ES)
Department of Ocean Engineering and Marine Sciences
Florida Institute of Technology
150 West University Blvd
Melbourne, FL 32901

US Army Engineer Research and Development Center
Coastal and Hydraulics Laboratory
3909 Halls Ferry Road
Vicksburg, MS 39180-6199

8. PERFORMING ORGANIZATION REPORT NUMBER
ERDC/CHL TR-22-5

9. SPONSORING/MONITORING AGENCY NAME(S) AND ADDRESS(ES)
US Army Engineer Research and Development Center
3909 Halls Ferry Road
Vicksburg, MS 3910-6199

10. SPONSOR/MONITOR'S ACRONYM(S)
ERDC

11. SPONSOR/MONITOR'S REPORT NUMBER(S)

12. DISTRIBUTION/AVAILABILITY STATEMENT
Approved for public release; distribution is unlimited.

13. SUPPLEMENTARY NOTES
Funding Account Code U4362900; AMSCO Code 06000

14. ABSTRACT

Navigation channels are periodically dredged to maintain safe depths. Dredged sediment was historically placed in upland management areas or in offshore disposal areas. Florida state law prohibits placement of beach fill sediment that contains more than 10% by weight of silt and clay, which is typically a characteristic of dredged material. An alternative is placement in a nearshore berm. Some potential benefits of nearshore berms include wave energy dissipation, reduced cost of dredging and shore protection, and possible onshore movement of the berm material. This study considers sediment distribution, morphological evolution, sediment transport, and shoreline trends along Fort Myers Beach, Florida, related to the nearshore berm constructed in August 2016. Due to timing of the field study, this report also includes information on the influence of a major hurricane that impacted the area. The overall conclusion of this study is that the dredge-sourced sediment in the berm performed as expected. Within 2 years, the berm adjusted to the shoreface environment, maintained a large part of its original volume, and contributed to protection of the beach and shoreline. The impact of Hurricane Irma included a shift in sediment textures and a large but temporary increase in shoreface sediment volumes.

15. SUBJECT TERMS

Beach nourishment, Coastal sediments, Dredging spoil, Fort Myers (Fla.), Littoral drift, Sedimentation and deposition

16. SECURITY CLASSIFICATION OF:			17. LIMITATION OF ABSTRACT	18. NUMBER OF PAGES	19a. NAME OF RESPONSIBLE PERSON
a. REPORT	b. ABSTRACT	c. THIS PAGE			Douglas R. Krafft
Unclassified	Unclassified	Unclassified	SAR	92	19b. TELEPHONE NUMBER *(Include area code)* 601-634-6097